



Earth's surface oxygenation and the rise of eukaryotic life: Relationships to the Lomagundi positive carbon isotope excursion revisited

Mojtaba Fakhraee^{a,b,c,*}, Lidya G. Tarhan^{a,*}, Christopher T. Reinhard^{b,c}, Sean A. Crowe^d, Timothy W. Lyons^{c,e}, Noah J. Planavsky^{a,c}

^a Department of Earth and Planetary Sciences, Yale University, New Haven, CT, United States

^b School of Earth and Atmospheric Sciences, Georgia Tech, Atlanta, GA, United States

^c NASA Interdisciplinary Consortia for Astrobiology Research (ICAR), Alternative Earths Team, Department of Earth and Planetary Sciences, University of California, Riverside, Riverside, CA 92521, United States

^d Department of Earth, Ocean, and Atmospheric Sciences, University of British Columbia, Vancouver, British Columbia, Canada

^e Department of Earth and Planetary Sciences, University of California, Riverside, Riverside, CA 92521, United States

ARTICLE INFO

Keywords:

Earth's oxygenation
Lomagundi
Eukaryotes
Carbon isotope excursion

ABSTRACT

The availability of molecular oxygen shapes the size and structure of Earth's biosphere. Geological and geochemical records imply that, for most of the Precambrian (the entirety of Earth's history with the exception of the most recent 540 million years), atmospheric oxygen concentrations were only a fraction of that of the present. A notable exception occurred in the wake of the first major rise in atmospheric oxygen between ~2.3 and 2.0 billion years ago. This interval is characterized by the largest and longest-lived marine carbon isotope excursion in Earth's history, the Lomagundi, which was accompanied by a major reorganization of global biogeochemical cycles. Despite this prominent change in the Earth system, the cause(s) of this remarkable inferred rise and subsequent fall in atmospheric oxygen levels and the consequences—for both marine biogeochemical cycling and the emergence and radiation of eukaryotic life—remain underexplored. Importantly, there is no robust evidence for increased biological complexity or the emergence of organisms with high oxygen demands despite strong indications of a stable and well-oxygenated Earth system over the 100–300 million-year Lomagundi interval. This decoupling is in sharp contrast to oxygenation during the later Neoproterozoic and early Paleozoic Eras, which temporally coincided with the expansion of eukaryote-rich ecosystems, including the appearance and radiation of animals. Emerging evidence for strong and stable, albeit ultimately impermanent oxygenation in the Paleoproterozoic that was divorced from increases in evolutionary complexity substantially broadens our framework for reconciling environmental and biotic co-evolution through Earth's history. The lack of an obvious temporal link between this prominent Paleoproterozoic episode of long-lived and likely substantial oxygenation and physiological and ecological diversification suggests that the former does not always foster the latter.

1. An overview of Earth's oxygenation

The chemistry of Earth's ocean-atmosphere system is fundamentally controlled by biological activity (Knoll et al., 2012; Wacey et al., 2008). Notably, the activity of Earth's biosphere led to atmospheric oxygen (O₂) concentrations that are today many orders of magnitude higher than possible on a planet devoid of life (Fischer et al., 2016; Lyons et al., 2014, 2021). Indeed, the transformation of Earth's atmospheric composition through oxygen release by primary producers (i.e., cyanobacteria, algae, and plants) over the past few billion years provides a

striking and instructive example of life fundamentally reshaping a planetary surface. Such oxygenation was certainly an essential condition for the emergence of large, complex aerobic organisms such as the human species and the wide diversity of animals that preceded that step (Catling et al., 2005; Fischer et al., 2016; Knoll et al., 2012; Knoll and Nowak, 2017). As a result, reconstructing Earth's planetary evolution, including the history of oxygenation, provides insight into our own origins while also informing efforts to identify planetary biosignatures that may be used in the search for life beyond our solar system (Schwieterman et al., 2018). However, many basic aspects of Earth's atmospheric

* Corresponding authors at: Department of Earth and Planetary Sciences, Yale University, New Haven, CT, United States.

E-mail addresses: mojtaba.fakhraee@yale.edu (M. Fakhraee), lidya.tarhan@yale.edu (L.G. Tarhan).

history and the interplay of atmospheric and biotic evolution are still actively debated or are known from only broad-brush approximations.

All known examples of complex multicellularity require oxygen at some stage of their life cycle (Butterfield, 2009; Knoll and Nowak, 2017). It is thus fair to say that oxygenation of Earth's surface environments must, at some level, have paved the way for biological complexity (Knoll and Nowak, 2017; Knoll and Sperling, 2014). Nonetheless, there are conflicting views regarding: (1) how to reconstruct trends in surface oxygen levels over the past three billion years of Earth and life history and (2) the extent to which oxygenation may have been driven by or, alternatively, may have facilitated biotic innovations and ultimately the emergence and radiation of complex life (Cole et al., 2020; Knoll and Nowak, 2017). There is now compelling evidence that Earth's atmosphere first became well-oxygenated around 2.4 billion years ago (Ga)—during what is referred to as the Great Oxidation Event (GOE) (Bekker et al., 2004; Holland, 2006; Lyons et al., 2014, 2021). The emergence of oxygenic photosynthesis was an evolutionary singularity that must have preceded the GOE (Avila et al., 2013; Planavsky et al., 2014a; Tice and Lowe, 2004). However, the question of how proximal the emergence of oxygenesis was to the GOE's dramatic increase in oxygen levels has been a topic of ongoing debate (Knoll and Nowak, 2017; Mills et al., 2022). A range of studies has proposed that oxygenic photosynthesis evolved more than 500 million years prior to the GOE and that environmental factors—rather than the direct evolution of oxygenic photosynthesis—may have played a more direct role in the initiation of the GOE (Awramik, 1992; Boden et al., 2021; Crowe et al., 2013; Fournier et al., 2021; Jabłońska and Tawfik, 2021; Johnson et al., 2022; Planavsky et al., 2014a). Others, however, have suggested a relatively late-stage emergence of oxygenic photosynthesis, immediately preceding and directly precipitating the GOE as Earth's first major episode of oxygenation (e.g., Fischer et al., 2016; Slotznick et al., 2022; Soo et al., 2017).

Reconstructions of Earth's oxygenation history have traditionally included a second, appreciable climb in oxygen levels roughly coincident with the rise of animals and radiation of macrophyte algae, between 800 and 540 million years ago—in what is now often referred to as the Neoproterozoic Oxidation Event (NOE) (e.g., Och and Shields-Zhou, 2012; Shields-Zhou and Och, 2011; reviewed in Lyons et al., 2021). However, most proxy records do not point toward a single, stepwise increase in oxygen levels over this interval (Canfield et al., 2008; Frei et al., 2013; Guilbaud et al., 2015; Kimura and Watanabe, 2001; Pogge Von Strandmann et al., 2015; Sperling et al., 2015; Wallace et al., 2017), indicating instead a complex and protracted history of dynamic oxygenation. Although there has been a surge of work over the past two decades, fueled largely by the development and application of a suite of new redox proxy systems, this work has not fostered community consensus regarding the detailed spatial and temporal trajectory of Earth's atmospheric evolution during the late Neoproterozoic. It remains unclear, in many cases, whether apparent discrepancies between proxy records reflect real, primary variability across short timescales and within discrete environments, or whether this disagreement instead reflects fundamental issues with proxy data interpretation and the unrecognized possible influence of local factors. Deciphering the utility of redox proxies and the robustness of individual proxy records must, therefore, be an integral component of reconstructing surface oxygenation and assembling a realistic account of Earth's history going forward. Nonetheless, despite uncertainties regarding the exact timing, magnitude, and directionality of oxygenation during the Neoproterozoic and across the Neoproterozoic-Cambrian transition, the majority of proxy records strongly support that Neoproterozoic and early Paleozoic oxygen levels were substantially higher than those of the Mesoproterozoic, suggesting that surface oxygen levels and eukaryote-rich ecosystems rose roughly concurrently across this interval (e.g., Canfield et al., 2007; Gross and Bhattacharya, 2010; Knoll and Nowak, 2017; Stamati et al., 2011; Lyons et al., 2021). We include these details about the Neoproterozoic, despite the overarching focus of the paper on earlier

oxygenation and its possible relationship with life, because questions that have recently risen to the fore of discussions regarding Paleoproterozoic evolution mirror those that have long been central to Neoproterozoic debates. We suggest that joint consideration of both Paleoproterozoic and Neoproterozoic episodes of oxygenation may provide critical insights into the commonality of Precambrian patterns of environmental and biotic co-evolution.

There are two commonly discussed but opposing views of the drivers of this second increase in Earth's oxygenation: (1) that this oxidation was driven by biotic innovations like, for example, the emergence and radiation of eukaryotic phytoplankton (Butterfield, 2009; Lenton et al., 2014; Logan et al., 1995) or (2) that oxygenation was linked to a shift in solid Earth processes and that higher oxygen levels, in turn, helped facilitate the rise of more complex, eukaryote-rich ecosystems (Cole et al., 2020; Cox et al., 2018; Duncan and Dasgupta, 2017; Lyons et al., 2021; McKenzie et al., 2016; Olson et al., 2019). The basis for each of these conceptual models—that complex life and oxygenation, whether driver or response, are integrally linked—is straightforward. However, they represent fundamentally different views of the planetary-scale evolution of the biosphere and biogeochemical cycling. More oxygenated oceans could have enhanced biospheric energy fluxes on a global scale which, in turn, could have fostered the radiation of eukaryote-rich ecosystems including animal-dominated seafloor communities (e.g., Kipp and Stüeken, 2017). Alternatively, changes in the average size of phytoplankton, linked to shifts in ecology to more eukaryote-dominated communities combined with the generally larger size of eukaryotes, may have led to a redistribution of oxygen demand and enhanced carbon burial (Butterfield, 2009; Fakhraee et al., 2020; Lenton et al., 2014; Lenton and Daines, 2018; Logan et al., 1995; Tziperman et al., 2011). Over the long term, such enhanced carbon burial would cause greater net oxygen production and oxygenation of the ocean-atmosphere system. A logical extension of this framework is that oxygenation of oceans dominated by bacterial primary production could, prior to the emergence of larger and more complex modes of biological organization, have been hampered by what has been inferred to have been a relatively inefficient biological pump (Butterfield, 2009; Logan et al., 1995).

Here, we propose that new constraints on the evolving chemistry of Earth's early oceans and atmosphere can help us gauge the roles that biotic innovations may have played in driving major steps in Earth's environmental evolution, thus further exploring the degree to which life drove environmental history rather than the reverse. In particular, as we discuss below, the early Paleoproterozoic was characterized by a distinct Earth system state that experienced extensive oxygenation in the absence of eukaryotic life (e.g., Mänd et al., 2022). Further, this stable oxic Earth system state may have spanned hundreds of millions of years but lacks any robust evidence for an associated rise in biological complexity. This is in sharp contrast to the later Proterozoic and earliest Phanerozoic, which are characterized by a broad temporal correspondence between substantial changes in ocean-atmosphere oxygenation and the expansion of eukaryote-rich ecosystems, including the emergence of animals (e.g., Brocks et al., 2017; Isson et al., 2018; reviewed in Lyons et al., 2021). If Paleoproterozoic oxygenation, in contrast to Neoproterozoic–Paleozoic oxygenation, were indeed entirely decoupled from major developments in biological and ecological complexity, this would suggest that transformative environmental changes are not always reliant upon and instead may cause or even be entirely decoupled from cascading shifts in the structure of the biosphere. In this sense, the Paleoproterozoic provides a useful test case for interrogating the links between environmental and biotic change over our planet's history, and whether, how, and when those lessons extrapolate to younger times in Earth's history must be considered.

2. The Great Oxidation Event

There have been major additions and refinements to the available quantitative constraints on Earth's atmospheric evolution over the last

two decades. However, the broader narrative—that the chemistry of Earth's ocean-atmosphere system has evolved from being pervasively anoxic to being strongly oxygenated, and that this oxygenation was protracted—has remained unchanged over the past half-century. Readily observable sedimentary features—foremost the appearance of iron-enriched sandstones, known as “red beds,” have long provided compelling evidence for appreciable atmospheric oxygen in the early Proterozoic (Eriksson and Cheney, 1992; Roscoe, 1969). The first red beds occur near the Archean-Proterozoic boundary, and these have been inferred to signify the transition to an oxygenated atmosphere (Holland, 1984; Kuang et al., 2022; Roscoe, 1969). This view, initially grounded in sedimentological field observations, was subsequently reinforced by the recognition that sedimentary rocks deposited prior to (but not after) this transition record mass-independent fractionation in sulfur isotopes (MIF-S; e.g., Farquhar et al., 2000). Modeling and experimental results suggest that these signatures require very low atmospheric O_2 (Farquhar et al., 2000; Farquhar and Wing, 2003; Pavlov and Kasting, 2002). The sedimentary MIF-S signal persists until around 2.3 Ga, though some signals captured in sedimentary rocks deposited between 2.45 and 2.31 Ga may reflect crustal recycling of MIF-S signals produced before this time and/or fluctuation in the production of MIF-S (Poulton et al., 2021; Reinhard et al., 2013; Uveges et al., 2023), suggesting that initial atmospheric oxygenation may have in fact taken place as early as between 2.5 and 2.48 Ga (Izon et al., 2022; Killingsworth et al., 2019; Philippot et al., 2018). However, a number of recent studies have suggested the alternative possibility of an extended period of periodic swings in oxygen over this interval (Poulton et al., 2021).

Vigorous debate over the relationship between the GOE and the emergence of oxygenic photosynthesis continues (Fischer et al., 2016; Soo et al., 2017; Ward et al., 2019). A number of studies have suggested, on the basis of geological, molecular, and geochemical proxy data (e.g., redox-sensitive elements, sulfur isotope systematics, phylogenetic analyses), that oxygenic photosynthesis and localized oxygen production emerged well before—perhaps even 500 million years prior to—the onset of the GOE (Crowe et al., 2013; Czaja et al., 2012; Fakhraee et al., 2018; Jabłońska and Tawfik, 2021; Kendall et al., 2010; Olson et al., 2013; Ossa Ossa et al., 2016, 2018; Ostrander et al., 2019, 2021; Planavsky et al., 2014a). These proxy records, like all proxy systems, rely on assumptions that may be difficult to test directly, and all Archean rocks have experienced extensive diagenesis and burial alteration that often mask primary signals. There are certainly cases where secondary alteration may have confounded putative signals of early oxygenesis (e.g., Albut et al., 2019). In the most extreme scenario, opposing views have argued that all these signals for early (pre-GOE) oxygenesis should be attributed to such secondary processes (Fischer et al., 2014; Rasmussen and Muhling, 2019). Regardless, there are several records that are widely agreed to be robustly linked to at least local oxygen production and thus indicate that cyanobacteria evolved well before the GOE. For example, the 2.9 Ga Pongola Supergroup (Wilson and Zeh, 2018) hosts sedimentary Mn deposits of meter-scale thickness that have been attributed to an active Mn oxide shuttle from ocean waters to the sediment pile (Ossa Ossa et al., 2018). Given that Mn oxides are easily reduced by a wide range of reductants, including ferrous iron, these enrichments, and associated Mo isotope signatures, most parsimoniously indicate the presence of fully oxygenated shallow shelf settings—and thus provide compelling evidence for early biological oxygen production (see Ostrander et al., 2019; Planavsky et al., 2014a).

Further, these Mn enrichments are stratigraphically continuous in rocks lacking any petrographic evidence for either extensive fluid flow or extensive alteration. It is therefore challenging to envision credible scenarios in which these enrichments, and their associated Mo isotope signatures (Planavsky et al., 2014a), could be linked to secondary alteration and, perhaps not surprisingly, none have been proposed. Records for early oxygen production during the Archean are by no means confined to the Pongola; as we discuss in greater detail below, several other successions, varying between 2.5 and 2.7 Ga in age, have

yielded multiple independent lines of evidence (e.g., redox-sensitive elements such as Mn, Fe, and Mo) for oxygen production, some of which are similarly characterized by a lack of evidence for extensive alteration (Czaja et al., 2012; Garvin et al., 2009; Kendall et al., 2010; Ostrander et al., 2019). Molecular clocks have also been used to constrain the emergence of oxygenic photosynthesis. However, these too have historically provided conflicting estimates for the timing of the emergence of this evolutionary singularity and, moreover, are generally associated with very large uncertainties (e.g., Battistuzzi et al., 2004). Some of the most recent efforts, however, have dated the emergence of key components of the oxygenic photosystem to the Mesoarchean, well before the GOE (see for example Boden et al., 2021; Cardona et al., 2019; Magnabosco et al., 2018). Basic aspects of Archean biotic and environmental evolution have long been at the center of debate regarding the evolution of Precambrian Earth systems (Holland, 1984; Ohmoto et al., 2006). However, views initially touted decades ago (Holland, 1984) continue to garner support: the Archean atmosphere was largely anoxic, and biological oxygen production likely evolved well before the initial transition to an oxygenated atmosphere (Fournier et al., 2021; Lyons et al., 2021; Planavsky et al., 2014a).

In a seminal paper, Cloud (1965) proposed that the Earth experienced a gradual and progressive rise in surface oxygen concentrations, from an initial increase in atmospheric oxygen to the emergence of animals (Cloud, 1965). This progressive oxygenation model, however, was not firmly grounded in mechanisms or records. Although the trajectory of oxygenation is still being pieced together and debated (Campbell and Allen, 2008; Lyons et al., 2014), there are now numerous studies suggesting that this model of a unidirectional and progressive rise in oxygen levels cannot be applied to Earth's middle history (from around 2.5 to 0.5 Ga). Perhaps the most straightforward critique of Cloud's progressive model is that extensive scrutiny of this interval over the past few decades has failed to yield empirical support for a monotonic and linear increase in atmospheric O_2 levels (Lyons et al., 2014). Instead, a non-linear, two-step oxygen model with an initial oxygen rise during the GOE followed later by another during the Neoproterozoic–early Paleozoic, concurrent with the rise of animals—is now commonly invoked and has been garnering further empirical and modeling support (Alcott et al., 2019; Lyons et al., 2014).

3. The Lomagundi

Below we focus on geochemical proxies that are commonly used to track pronounced differences between Paleoproterozoic and Mesoproterozoic redox states and pO_2 levels. Although questions remain concerning how to best piece together these records, our discussion encompasses nearly all published geochemical data pertaining to this question and interval. Below we describe the current state of knowledge regarding marine and atmospheric redox shifts across this interval; discuss insights gained by the synthesis of these datasets; and highlight areas of continuing uncertainty that should, in our view, be regarded as key targets for future study.

3.1. Insights from carbon isotopes

The most prominent example of a likely rise and subsequent fall in Paleoproterozoic oxygen levels occurs immediately after the initial enduring oxygenation of the atmosphere as delineated by permanent loss of MIF-S—in what is often treated as a continuation of the GOE (Bekker, 2019; Poulton et al., 2021). Carbon isotope data ($\delta^{13}C$) have, historically, provided the first indication that the coupled carbon and oxygen cycles behaved dynamically during the Paleoproterozoic. Specifically, $\delta^{13}C$ records suggest that massive amounts of organic carbon burial—and associated oxygen release—occurred in the aftermath of the initial rise of atmospheric oxygen (Karhu and Holland, 1996). Within a stratigraphically short interval, following the loss of the MIF-S signal, extremely positive carbon isotope values ($>10\text{‰}$) are recorded in

shallow-water carbonates of the Duitschland Formation in South Africa (Bekker et al., 2001). This record should, in the traditional carbon cycle framework (Karhu and Holland, 1996; Kump and Arthur, 1999), reflect an episode of highly elevated organic carbon burial, which should have led to a similarly large net oxygen flux to the ocean-atmosphere system. These anomalously positive carbon isotope values appear to be a prominent feature of the lower Paleoproterozoic record (Bekker and Holland, 2012; Schidlowski et al., 1976), with the positive carbon isotope signal recorded in over 15 different broadly coeval sedimentary rock successions worldwide (Fig. 1). One notable example of this persistent, positive carbon isotope signal (and the unit in which this record was first discovered) is the Lomagundi Group of Zimbabwe, which has since lent its name to this extended interval of carbonate deposition with anomalously positive carbon isotope values—the

Lomagundi Excursion. The initiation of the Lomagundi postdates 2.316 ± 0.007 billion years ago (Ga) (Transvaal Supergroup, South Africa (Hannah et al., 2004)) and predates 2.221 ± 0.007 Ga (Palokivalo Formation, Scandinavia (Pertunnen and Vaasjoki, 2001)). In the Pechanga Greenstone Belt, Fennoscandia, the termination of the Lomagundi has been assigned a maximum age of 2.058 ± 0.002 Ga (Melezhik et al., 2007). Using conservative age ranges, these observations suggest that the Lomagundi was somewhere between 160 and 260 million years in duration (Martin et al., 2013).

In the standard interpretive framework for carbon isotope excursions, the Lomagundi would have led to the release of up to ~ 20 times the modern atmospheric reservoir of O_2 (Karhu and Holland, 1996), and this should have driven appreciable oceanic and atmospheric oxygenation. There has, however, been an increasing realization that many of

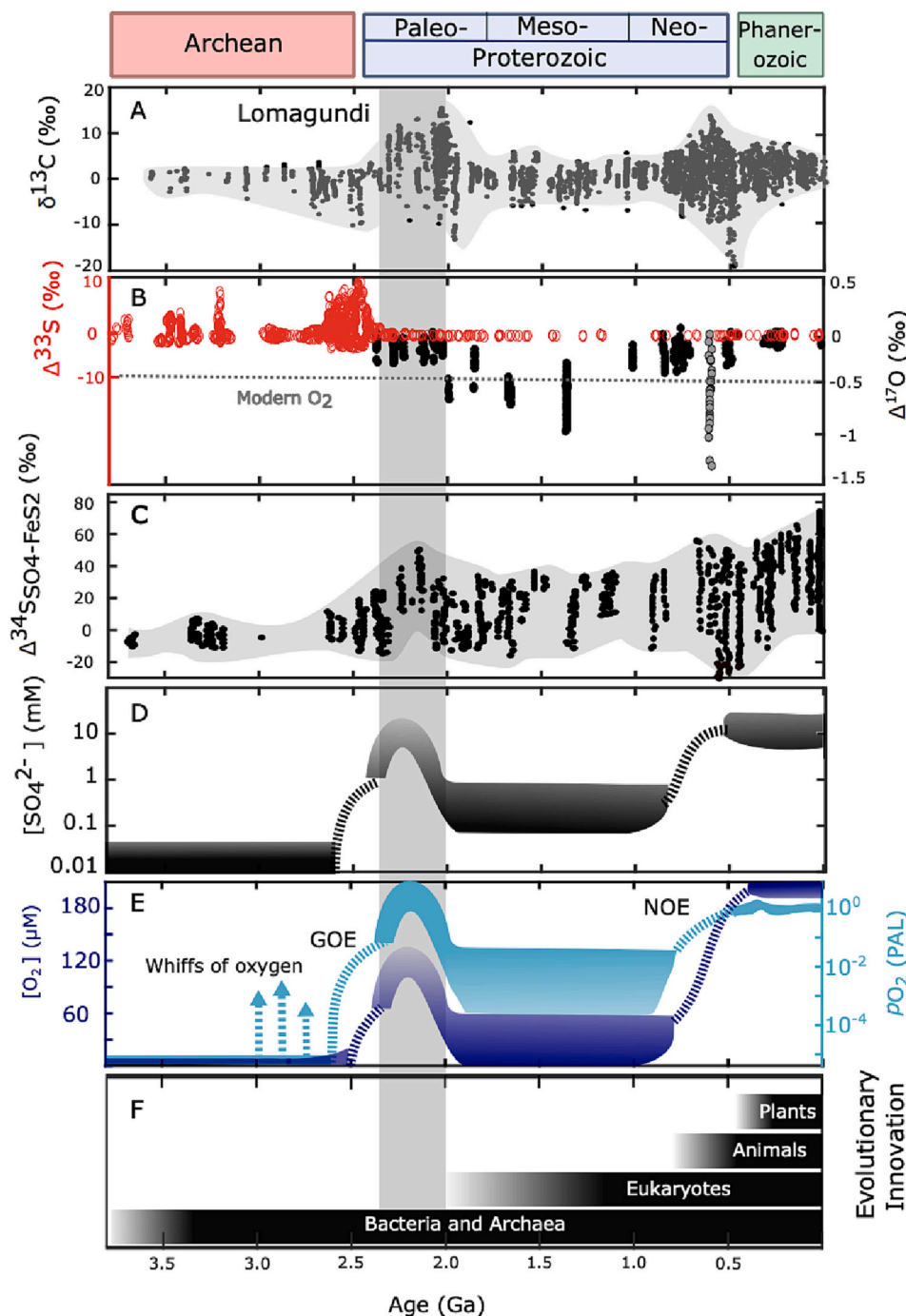


Fig. 1. Major geochemical changes and the emergence of key biological groups over the past four billion years of Earth's history. (A) Carbon isotope ($\delta^{13}C$) records in carbonate minerals; (B) oxygen ($\Delta^{17}O$) and sulfur ($\Delta^{33}S$) isotope signatures of sedimentary sulfate and sulfide minerals, which respectively constrain oceanic productivity and atmospheric anoxia; (C) the difference in the isotopic composition of seawater sulfate and sedimentary pyrite ($\Delta^{34}S_{SO_4-FeS_2}$). Increase in $\Delta^{34}S_{SO_4-FeS_2}$ can be explained by higher sulfate availability; (D) seawater sulfate levels—oxic oceans are needed for the growth of the marine sulfate reservoir; (E) shallow marine and atmospheric oxygen concentrations; and (F) the timing of the emergence of major biological groups. The disappearance of $\Delta^{33}S$ anomalies from the rock record marks the first major rise in atmospheric oxygen, known as the Great Oxidation Event (GOE). High $\delta^{13}C$, $\Delta^{17}O$, and sulfate during the Lomagundi (denoted, in all panels, by the vertical grey bar) strongly suggest an Earth system in which oxygen levels were elevated, potentially even to extents comparable to the modern Earth. Despite favorable environmental conditions during the Lomagundi, fossil and geochemical archives indicate that multicellularity did not emerge until well after this time, during the later Proterozoic. The grey circles in (B) correspond to $\Delta^{17}O$ values recorded from deposits formed during the Neoproterozoic Snowball Earth glaciations (Crockford et al., 2019). Sources for these data are cited in the main text.

the fundamental assumptions underlying the classic carbon isotope framework are problematic (Geyman and Maloof, 2019; Hodgskiss et al., 2023; Mayika et al., 2020; Miyazaki et al., 2018; Prave et al., 2022). The amount of organic carbon burial per unit time inferred from a positive carbonate carbon isotope value is dependent on the duration of the carbon isotope excursion, as well as ambient atmospheric oxygen levels. The latter dictates the extent of organic carbon oxidation, while the former determines the amount of ‘anomalous’ (e.g., ^{13}C -enriched) carbon recycled from sedimentary rocks back into the ocean-atmosphere system. Taking these factors into account, there are multiple non-unique interpretations of the Lomagundi positive carbon isotope excursion. For instance, recent estimates for the average rate of organic carbon burial through the Lomagundi range from less than half to just over twice the modern burial flux (e.g., Miyazaki et al., 2018).

There is also growing acceptance that shallow-water carbonates commonly do not track the carbon isotope composition of open-ocean dissolved inorganic carbon (DIC) (Geyman and Maloof, 2019, 2021; Hodgskiss et al., 2023). Due to surface primary production on nutrient-rich productive margins and platforms, modern shallow-water carbonates are characterized by highly variable and commonly enriched carbon isotope values (up to $>6\%$ heavier than deep-ocean carbonates, which today predominantly consist of the remains of open-ocean-dwelling calcifying plankton) (Geyman and Maloof, 2019; Swart, 2015; Swart and Eberli, 2005). Generally, in shallow settings, the exchange of carbon between organic and inorganic pools is governed by carbonate precipitation and dissolution, atmospheric gas exchange, and photosynthesis and respiration. In such environments, photosynthesis is the main driver of perturbations to the carbonate system during the day, as the uptake of isotopically light carbon leaves the surrounding DIC reservoir correspondingly isotopically enriched. During the night, the system moves to respiration (see Geyman and Maloof, 2019). However, due to inefficiencies in respiration as well as organic matter export, there is a net imbalance in favor of production. As a result, during a single (24-hour) diurnal-nocturnal cycle, the localized carbon exchange flux

between organic and inorganic pools can outcompete the carbonate burial flux by over a factor of 20, resulting in a carbon isotope offset between the relatively enriched isotopic composition of carbonate in shallow (production-dominated) ocean and relatively less enriched (commonly lower-productivity) open-ocean settings (Fig. 2) (Geyman and Maloof, 2019). If this process similarly affected carbonates recording the Lomagundi Excursion, this may suggest that traditional calculations of the oxygen flux (e.g., Karhu and Holland, 1996) associated with the Lomagundi may need to be revisited.

3.2. Insights from triple oxygen isotopes

Although there is still agreement that organic carbon burial is likely to be the main factor driving shifts in atmospheric oxygen levels through the Precambrian (e.g., Canfield, 2021; Miyazaki et al., 2018; Planavsky et al., 2022b), there is an emerging consensus that we must leverage additional records, beyond that of carbon isotopes, to accurately reconstruct ancient biospheric oxygen production fluxes and their corresponding impact on atmospheric oxygen. Our knowledge of Archean atmospheric oxygen levels has been transformed by MIF-S work, which directly tracks atmospheric processes that can be linked to atmospheric oxygen levels in a nearly quantitative framework. Mass-independent O isotope fractionations—which can be recorded in marine sulfate minerals—may provide an analogous and perhaps more direct approach toward directly tracking atmospheric oxygen levels (Crockford et al., 2018; Planavsky et al., 2018). Photochemical reactions in the stratosphere result in the production of ozone (O_3) with a mass-independent oxygen isotope fractionation, during which O_3 becomes enriched in ^{17}O , whereas O_2 becomes depleted in ^{17}O (Hayles et al., 2016; Thiemens, 2006; Thiemens and Heidenreich, 1983; Wen and Thiemens, 1993). Depletions and enrichments in ^{17}O are termed triple-oxygen isotope anomalies and, similar to MIF-S signals, are expressed as deviations from a strictly mass-dependent fractionation ($\Delta^{17}\text{O} = \delta^{17}\text{O} - 0.5305(\delta^{18}\text{O}) \neq 0$). Experimental studies show that the magnitude of the $\Delta^{17}\text{O}$ signal in

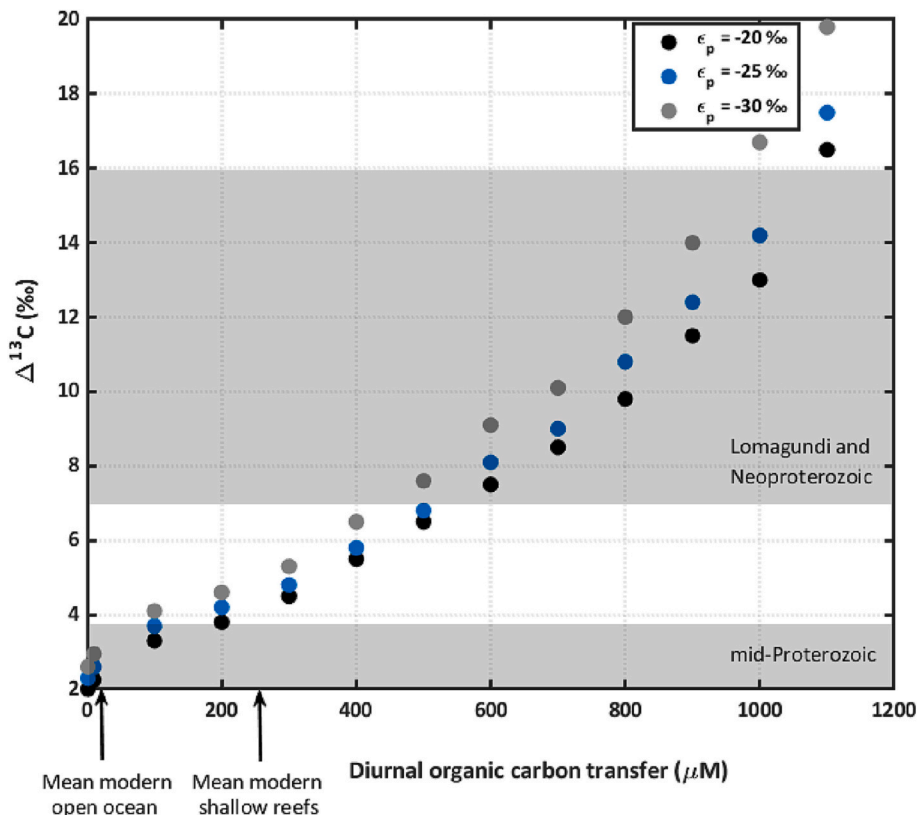


Fig. 2. The magnitude of carbonate $\delta^{13}\text{C}$ enrichment, relative to open-ocean DIC $\delta^{13}\text{C}$ (i.e., $\Delta^{13}\text{C}$) as a function of photosynthetic forcing in a shallow-water carbonate system (Geyman and Maloof, 2019). Arrows on the x-axis correspond, respectively, to average diurnal organic carbon transfer in the modern open ocean and modern shallow marine reefs; ϵ_p denotes various fractionations associated with photosynthetic carbon uptake. The upper grey box denotes maximum $\delta^{13}\text{C}$ in individual sections of Lomagundi carbonates; the lower grey box denotes mid-Proterozoic values. Lomagundi positive carbon isotope values can be reproduced by models if diurnal organic carbon transfer was two to six times higher than in the modern oceans, suggesting that the Lomagundi oceans must have been highly productive.

atmospheric oxygen is controlled by the reaction between oxygen atoms and carbon dioxide molecules in the stratosphere and other chemical species that affect heavy oxygen isotope values. Based on these results, the $\Delta^{17}\text{O}$ signal in atmospheric O_2 is proportional to CO_2 partial pressure ($p\text{CO}_2$) (Thiemens, 2006; Thiemens and Heidenreich, 1983; Wen and Thiemens, 1993). Oxygen molecules with MIF signals transported from the stratosphere would also be mixed with biologically produced oxygen (i.e., from marine primary production) in the troposphere that carries an essentially mass-dependent fractionation signal (0‰). The biospheric flux of oxygen is viewed to be approximate to the strength of gross primary production (GPP), meaning that the $\Delta^{17}\text{O}$ signal would also represent the oxygen flux through GPP (Luz et al., 1999). We can pursue archives of this relationship through preserved sulfate geochemistry. Within this framework, the $\Delta^{17}\text{O}$ value of sulfate minerals depends on three main factors: (1) atmospheric oxygen levels, (2) atmospheric carbon dioxide levels, and (3) the gross oxygen flux from the biosphere. The net effect of these factors today produces a $\Delta^{17}\text{O}$ value of around -0.47‰ (Pack et al., 2017). In this light, the extent of biospheric recycling of $\Delta^{17}\text{O}$ anomalies and atmospheric oxygen levels are directly linked. Although a single $\Delta^{17}\text{O}$ value may theoretically be produced via multiple pathways (see Liu et al., 2021), consideration in a statistical framework of the range of reasonable boundary conditions provides one means of limiting the number of plausible Earth states for any given $\Delta^{17}\text{O}$ value (e.g., Planavsky et al., 2018).

Considerable effort has recently been devoted to generating a new

sulfate mineral $\Delta^{17}\text{O}$ record through Earth's history (Fig. 1). Sulfates from the Lomagundi (from units ranging in age from 2.3 to 2.0 Ga) and the Neoproterozoic (0.8 to 0.55 Ga), Snowball Earth events excepted because of signals controlled by anomalous CO_2 levels (Bao et al., 2008), are characterized by statistically similar $\Delta^{17}\text{O}$ values (-0.26 ± 0.10 and -0.22 ± 0.08 , respectively) (Crockford et al., 2019). In contrast, sulfates from the mid-Proterozoic (1.8 to 0.8 Ga) are characterized by $\Delta^{17}\text{O}$ values (-0.65 ± 0.22) much lighter than those found during either the Lomagundi or the late Proterozoic (Crockford et al., 2018, 2019; Hodgskiss et al., 2019). These new $\Delta^{17}\text{O}$ records indicate that the mid-Proterozoic represents an Earth system state that was distinct from those at either the beginning or the end of the Proterozoic. An exciting avenue for future work will be efforts to translate $\Delta^{17}\text{O}$ values into quantitative estimates of atmospheric $p\text{O}_2$ (Liu et al., 2021).

3.3. Insights from nitrogen and phosphorus cycling

Changes in the cycling of nitrogen and phosphorus, as essential elements for marine productivity, can offer insight into changes in the redox state during the Lomagundi. For instance, a change in the isotopic composition of nitrogen in the rock record can indicate whether marine nitrification and denitrification, as regulated by seawater oxygen levels, were robustly operating during this interval (Stüeken et al., 2015, 2016). Under predominantly anoxic conditions, nitrogen is fixed into a reduced form of nitrogen (e.g., NH_4) with a minimal isotopic fractionation (e.g.,

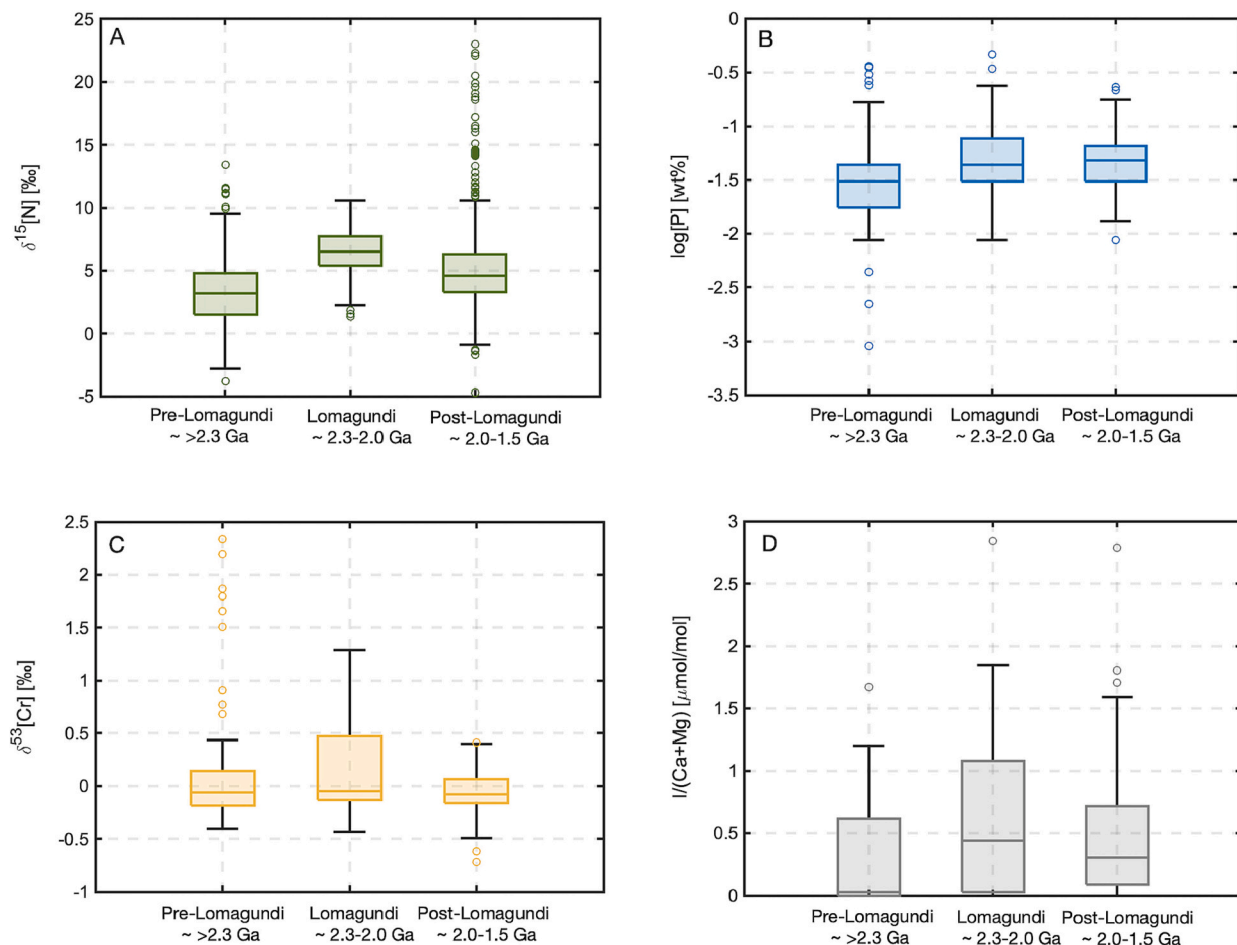


Fig. 3. Results from analysis of additional geochemical proxies from strata deposited before, during, and after the Lomagundi interval. Panels A, B, C, and D show, respectively, variations in the bulk isotopic composition of nitrogen, phosphorus content, the isotopic composition of chromium, and iodine content in stratigraphic records deposited before, during, and after the Lomagundi. The compiled data are from Hardisty et al. (2014, 2017); Kipp et al. (2018); Kipp and Stüeken (2017); Mänd et al. (2022); Planavsky et al. (2022a); Reinhard et al. (2017); and Stüeken et al. (2015, 2016). These geochemical proxy results, altogether, point toward an increase in oxidant levels in the ocean-atmosphere system during Lomagundi. Such an increase in oxidant levels, however, did not give rise to eukaryotic life.

Stüeken et al., 2016). Under oxic conditions, this reduced nitrogen can be readily oxidized into nitrate, a process known as nitrification (e.g., Ward et al., 2011). Nitrate produced in this manner can again become reduced into N_2 gas in low-oxygen marine waters through the “denitrification” process, thereby closing the N cycle (Canfield et al., 2010). Repeated coupled nitrification and denitrification would result in isotopically heavier nitrogen in the residual nitrate pool and heavier $\delta^{15}N$ values in marine organic matter (Stüeken et al., 2015, 2016). The isotopic composition of nitrogen in stratigraphic records spanning the Lomagundi has been inferred to reflect the presence of aerobic nitrogen cycling (Fig. 3a). Specifically, $\delta^{15}N$ values reported from Paleoproterozoic-aged samples are characterized by consistently positive $\delta^{15}N$ values (Kipp et al., 2018). The range of observed $\delta^{15}N$ values is well above the values expected for nitrogen-fixation-dominated systems (-2% to $+1\%$) and can be explained by active aerobic nitrogen cycling in the surface ocean where coupled nitrification and denitrification would have led to a positive excursion in $\delta^{15}N$ (Kipp et al., 2018; Stüeken et al., 2016). The presence of aerobic nitrogen cycling during the Lomagundi has been corroborated by more recent studies, which have likewise documented positive $\delta^{15}N$ values and interpreted these to reflect nitrate-replete and highly oxygenated conditions in continental shelf settings (Ossa Ossa et al., 2022).

Available data on phosphorus abundances in Lomagundi-aged records provide further support for an oxygenated surface ocean. Compilations of sedimentary phosphorus abundances through time show an increase—albeit not a very pronounced one—in phosphorus availability in the ocean during the Lomagundi (Fig. 3b) (Kipp and Stüeken, 2017; Planavsky et al., 2022a; Reinhard et al., 2017). High phosphorus abundances in marine shales can be explained by enhanced nutrient fluxes to the oceans and/or efficient recycling of phosphorus within the oceans (Hao et al., 2021; Kipp and Stüeken, 2017). Notably, under oxic conditions, most of the organic biomass produced in the photic zone would be degraded through heterotrophy in the surface oceans, resulting in relatively efficient recycling of phosphorus in the surface ocean (Kipp and Stüeken, 2017). Efficient P recycling would, in turn, lead to higher rates of primary production, driving higher oxygen production in the surface oceans (Kipp and Stüeken, 2017; Laakso and Schrag, 2019). This scenario is also consistent with a decrease in sedimentary C to P ratios during the Lomagundi (Kipp and Stüeken, 2017). Another potential driver of increased phosphorus availability during the Lomagundi is enhanced mineral-mediated transport of phosphorus to the oceans (Hao et al., 2021). Specifically, recent experimental work has highlighted the importance of kaolinite [$Al_2Si_2O_5(OH)_4$] in transporting particulate phosphorus to the oceans (Hao et al., 2021). Accordingly, at higher rates of weathering and high kaolinite content during the Lomagundi, the transport of phosphorus to the oceans would have been amplified, driving increased productivity and oxygen production in the surface oceans (Hao et al., 2021). These findings corroborate those of previous studies (e.g., $\Delta^{17}O$ records, as discussed above) that have likewise suggested that the Lomagundi ocean was highly productive (e.g., Hodgskiss et al., 2019).

3.4. Insights from marine sulfur cycling proxies

Sulfate is the most abundant oxidant in the modern oceans, but its abundance in seawater has varied dramatically over Earth's history in ways that, in a first-order sense, track biospheric oxygen levels. As such, temporal changes in marine sulfur cycling have been explored via various geochemical proxies to reconstruct the evolution of Earth's surface oxidation. There are multiple lines of evidence that sulfate levels increased during the Lomagundi (e.g., Blättler et al., 2018). For instance, Blättler et al. (2018) employed stratigraphic variability in calcium isotope ($\delta^{44}Ca$) values in evaporative facies of the ~2.0 Ga Tulomozero Formation evaporites to provide a more precise estimate of seawater sulfate concentrations. This approach rests on relatively straightforward principles—gypsum ($CaSO_4 \cdot 2H_2O$) precipitation induces a Ca isotope

fractionation, and the amount of Ca isotope distillation and fractionation across an evaporative sequence is, in turn, tied to the marine dissolved Ca/SO_4 ratio. Modeling this process—with additional constraints from the minerals formed during the evaporite sequence (carbonates, calcium sulfates, halite, and magnesium sulfates)—Blättler et al. (2018) estimated that marine sulfate levels during deposition of the Tulomozero Formation must have been >10 mM. Although there are uncertainties associated with this estimate because of the requirement for a number of assumptions, including the extent of connectivity of the evaporite-precipitating water body to the global ocean, this work in combination with other complementary studies strongly supports claims of substantial fluctuations in seawater sulfate levels from the μM range that characterized pre- and post-Lomagundi oceans to several mM during the event (Blättler et al., 2018; Crowe et al., 2014; Fakhraee et al., 2019; Planavsky et al., 2012).

The development of such a massive marine sulfate reservoir is important, given that mass balance modeling of the global sulfur cycle indicates that mM-level marine sulfate should require a well-oxygenated ocean (Fakhraee et al., 2019). This conclusion is consistent with reports of large sulfur isotope fractionation— $\Delta^{34}S_{SO_4-FeS_2}$ from coeval sulfate and pyrite sulfur isotope ($\delta^{34}S$) records—during the Lomagundi, indicating an active marine and terrestrial oxidative sulfur cycle (Fakhraee et al., 2019; Scott et al., 2014). Under widespread mid- and deep-ocean anoxia, if present, pyrite fluxes driven by water-column sulfate reduction would have been high enough to prevent the buildup of a large sulfate reservoir—unless primary productivity was much lower than that of the modern Earth ($< \sim 5\%$ of modern primary productivity; Fakhraee et al., 2019; Ozaki et al., 2019). Because $\delta^{13}C$ and $\Delta^{17}O$ records of the Lomagundi suggest that productivity levels were not especially low (Hodgskiss et al., 2019), the appreciable accumulation of marine sulfate during the Lomagundi implies limited deep-ocean anoxia.

It is possible, using a mass balance approach coupled with pyrite and sulfate $\delta^{34}S$ records, to estimate the relative fractions of the total sulfur flux to the oceans buried as pyrite and sulfate (Canfield and Farquhar, 2009; Halevy et al., 2012). Current $\delta^{34}S$ datasets reveal a clear signal for enhanced sulfate burial relative to pyrite burial during the Lomagundi, in strong contrast to the remainder of the Proterozoic (Kasten and Jørgensen, 2000; McDonnell and Buesseler, 2010). Moreover, the distribution of these data is remarkably similar to $\delta^{34}S$ data from the modern ocean, in which most of the sulfide produced by microbial sulfate reduction in anoxic sediments becomes re-oxidized (Kasten and Jørgensen, 2000; McDonnell and Buesseler, 2010; Tarhan et al., 2015). This calculation requires assumptions about the isotopic composition of the S input, and this value has considerable uncertainty that translates to uncertainties in the burial fluxes of pyrite and sulfate. However, even allowing for a reasonable yet broad range (~ 0 to 10%) of input S isotope values, the basic conclusion that the Lomagundi was characterized by elevated sulfate deposition remains robust.

3.5. Insights from iron cycling

Iron is another major element that acts as a strong lever on Earth's redox balance and, unsurprisingly, efforts to track iron cycling in the marine and terrestrial realms have played a major role in shaping our view of Earth's oxygenation. Ancient soil deposits (paleosols) that formed during the Lomagundi interval are—as for Phanerozoic soils—characterized by near-complete iron retention, that is, iron oxide formation in the upper soil profile (e.g., Beukes et al., 2002). In contrast, it has become increasingly clear that well-preserved mid-Proterozoic paleosols are marked by iron loss manifested in limited iron oxide abundance and thus low inferred formation and preservation in the upper soil profile (Colwyn et al., 2019; Mitchell and Sheldon, 2009, 2010). This relationship is commonly interpreted to indicate that mid-Proterozoic atmospheric oxygen levels were lower than $\sim 1\%$ PAL (e.g., as reviewed by Planavsky et al., 2018).

Although various proxy systems suggest prominent increases in the

oxidation of the shallow oceans during the Lomagundi, iron-based proxy records also suggest that deep-water anoxia persisted, at least locally, through the Proterozoic into the early Phanerozoic (e.g., Lyons et al., 2014; Sperling et al., 2015). The transport of dissolved iron into shallow marine settings is a traditional indicator of low (<1% PAL) atmospheric oxygen (Canfield, 2005). Iron formations are notably absent from stratigraphic successions recording the Lomagundi Excursion (Bekker et al., 2010). However, a return to widespread deposition of iron formations nearly worldwide, including in unambiguously wave-reworked, shallow-water marine settings at 1.88 Ga, arguably provides strong evidence for a return to low-oxygen conditions—in both the shallow and deep oceans—in the post-GOE and post-Lomagundi world (Fig. 4). There are, moreover, multiple marine successions characterized by additional geochemical signatures for shallow-water anoxia from 1.8 to 0.8 Ga, and these records provide the most striking indication that oxygen levels oscillated or potentially remained persistently low after the Lomagundi (Arnold et al., 2004; Cole et al., 2016; Shen et al., 2003; Tang et al., 2016). In particular, iron speciation records (i.e., the relative abundance of iron phases) in marine sedimentary rocks generally indicate a background state of pervasive marine anoxia, with episodes of local oxygenation, during extensive intervals of the mid-Proterozoic (Fig. 4) (Shen et al., 2003; Sperling et al., 2015; Tang et al., 2016; Wang et al., 2022).

3.6. Insights from redox-sensitive elements

The available data for the behavior of redox-sensitive elements during the Lomagundi points to an increase in the oxidation state of the ocean-atmosphere system across this interval. In particular, results from analyses of chromium (Cr) (Mänd et al., 2022), selenium (Se) (Kipp et al., 2017; Ossa Ossa et al., 2022), copper (Cu) (Chi Fru et al., 2016), arsenic (As) (Chi Fru et al., 2019), thorium (Th), and uranium (U) concentrations (Partin et al., 2013) and isotope values (Liu et al., 2019), suggest an enhancement in oxygen availability during the Lomagundi. For instance, Cr isotope measurements generated from a > 2400-m core from the Onega Basin (northwestern Russia), with an age of approximately 2.1–2.0 Ga suggest elevated atmospheric oxygen levels may have persisted in surface environments for at least 100 million years, during which seawater oxygen levels may have been higher than during the intervals either preceding or following the Lomagundi (Fig. 3c) (Mänd et al., 2022). A similar conclusion has been drawn from the characterization of Se isotope signatures from muddy lithologies of this age. Previous studies have proposed that a positive excursion in $\delta^{82/78}\text{Se}$ values in ca. 2.32–2.10 Ga offshore shales records an increase in

contemporaneous oxygen concentrations (Kipp et al., 2017). These datasets also corroborate observed changes in the isotopic composition of Cu in marine black shales (Chi Fru et al., 2016). More precisely, a shift from negative to positive copper isotopic compositions ($\delta^{65}\text{Cu}$) in organic carbon-rich shales, including correlation of the highest isotopic values with the Lomagundi interval (2.15–2.08 Ga), has been interpreted to reflect an increase in the oxidative weathering flux of Cu from the continents to the oceans (Chi Fru et al., 2016). Characterizations of As, Th, and U have further corroborated previous proposals that oxygen availability increased during the Lomagundi (Chi Fru et al., 2019; Liu et al., 2019). Notably, Th/U long-term records from arc volcanic rocks since 3.0 (Ga) reveal two major shifts in the Th/U values occurring at approximately 2.35 and 0.75 Ga, which are roughly consistent with a noticeable change in the oxidation state of the Earth during the Great Oxidation Event (GOE) and Neoproterozoic Oxidation Event (NOE), respectively (Liu et al., 2019). Mechanistically, highly oxic conditions would promote oxidation of water-insoluble U_4 to the water-soluble U_6 , which would then readily dissolve in seawater and become incorporated into altered oceanic crust. Subduction of this altered oceanic crust would result in the production of arc igneous rocks with low Th/U values (Liu et al., 2019). These data also suggest a shift to higher Th/U values near the end of the Lomagundi (~2.0 Ga), which have been attributed to a decrease in oxygen availability and a return to a predominantly anoxic ocean-atmosphere Earth system (Liu et al., 2019).

3.7. Insights from iodine records

The relative abundance of iodine in marine carbonates is another geochemical proxy that is commonly used to track the evolution of ocean oxygenation (e.g., Hardisty et al., 2014). Observations from modern anoxic settings indicate that, in the absence of molecular oxygen, the oxidized form of iodine, iodate (IO_3), is reduced to iodide (I^-) (Luther and Campbell, 1991; Wong and Brewer, 1977). This redox-dependent behavior of iodine along with a linear correlation between the abundance of carbonate-associated iodine and the dissolved IO_3 levels in the waters in which the carbonate forms, along with a relatively long residence time of iodine in the oceans (~300,000 years), have led to the wide use of carbonate I/Ca ratios as a proxy to track the oxidative capacity of the oceans (Lu et al., 2010). Reconstruction of long-term shallow marine carbonate I/Ca records suggests an increase in surface ocean oxygenation occurred during the Lomagundi (Fig. 3d) (Hardisty et al., 2014). While the exact correlation between dissolved oxygen and iodate levels is not well known and will require further scrutiny of iodine cycling in both oxic and anoxic modern settings, increase in the I/Ca

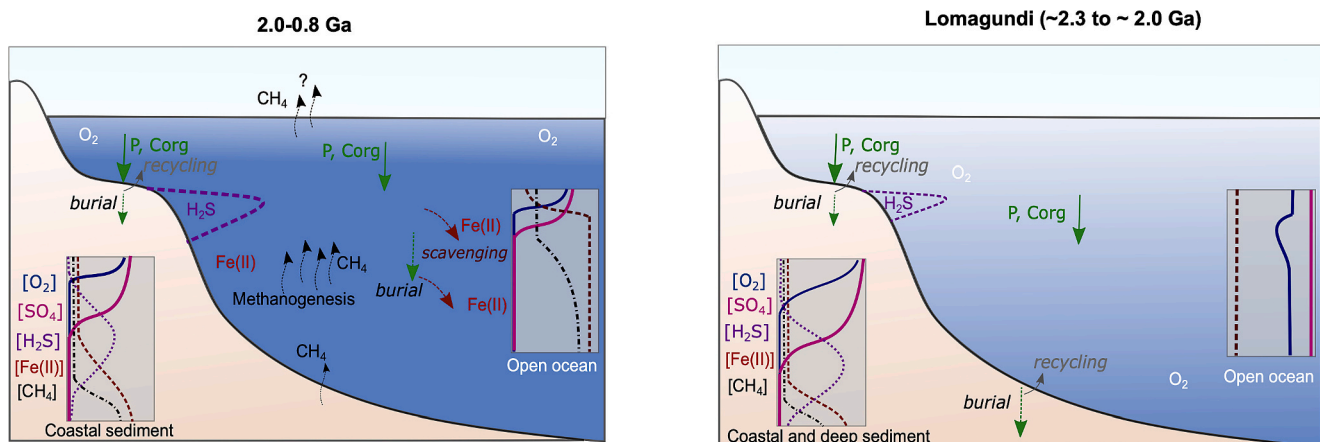


Fig. 4. Inferred changes in ocean redox state during the Proterozoic. The ocean-atmosphere system for most of the Proterozoic (left panel) was characterized by widespread iron-rich conditions, with inefficient cycling of phosphorus through Earth's biosphere due to iron scavenging and relatively low sulfate concentrations. During the Lomagundi (right panel), well-oxygenated conditions resulted in more efficient cycling of phosphorus, higher productivity, and more pervasive ocean oxygenation.

values of marine shallow carbonates are widely regarded to reflect increases in surface ocean oxygen availability (e.g., Hardisty et al., 2014, 2017). In sum, although aspects of particular proxy records remain areas of ongoing research, the data currently available from a wide range of proxy systems and lithological archives suggests that surface ocean oxygen levels increased during the Lomagundi.

4. The Post-Lomagundi World—return to low-oxygen conditions

Over the past few decades, a range of proxy records have emerged that point to an initial rise in Earth's surface oxygen levels during the Paleoproterozoic (as discussed above). Although the atmosphere remained permanently oxygenated following the GOE, the high-oxygen state that characterized the Lomagundi was apparently followed by a notable decrease in both atmospheric and marine oxygen levels. The deep oceans, in particular, returned to a state of widespread anoxia that was pervasive, though perhaps locally and regionally variable, through much of the remainder of the Proterozoic. Further, background low-oxygen conditions appear to have persisted well into the early to mid-Paleozoic (e.g., Sperling et al., 2015). Various studies have suggested that there may have been other swings in atmospheric oxygen levels during the Paleoproterozoic and Mesoproterozoic (Daines et al., 2017; Fralick et al., 2017; Gilleaudeau et al., 2016; Poulton et al., 2021). However, these have not, as of yet, been supported by diverse lines of evidence, nor are there currently data to suggest that such fluctuations would have come even close to rivaling the Lomagundi in magnitude or duration. Specifically, iron speciation, sulfur isotope, and chromium isotope analyses, as well as data from other redox-sensitive elements, have suggested fluctuation in atmospheric O₂ levels during the Paleoproterozoic and Mesoproterozoic (Fralick et al., 2017; Gilleaudeau et al., 2016; Poulton et al., 2021; Lyons et al., 2021). Notably, recent high-resolution iron speciation and sulfur isotope datasets generated from marine strata of the Transvaal Supergroup, South Africa, have been interpreted to reflect fluctuation in atmospheric oxygen levels, likely caused by oscillations in marine redox chemistry, from approximately 2.32 to 2.22 Ga (Poulton et al., 2021). These results have been recently challenged by a re-analysis of Transvaal strata from the same basin, using sulfur isotope systematics (Izon et al., 2022). But regardless of whether this trend is robust and primary in nature, such fluctuation is dwarfed by the size and duration of the Lomagundi.

As discussed above, a rich and growing body of work indicates that both the Lomagundi and the Neoproterozoic were characterized by comparably high atmospheric oxygen levels—in contrast to the low background oxygen levels of the Mesoproterozoic. Collectively, these datasets suggest convincingly that Earth has not undergone progressive and unidirectional oxygenation and that a simple two-step history likely overlooks appreciable dynamics in oxygenation across the Proterozoic Eon and into the Paleozoic Era. This realization has major implications for how we view the potential drivers and consequences of Earth's oxygenation and should be central to the discussion surrounding the links between ocean-atmosphere oxygenation and the emergence of biological complexity, as we explore in greater detail below.

5. Is large complex life an essential prerequisite for oxygenation?

Many researchers have suggested that oxygenation of the Neoproterozoic–Cambrian oceans was causally linked to the radiation of eukaryotes (Butterfield, 1997, 2009; Lenton et al., 2014; Lenton and Daines, 2018; Logan et al., 1995). Specifically, it has commonly been suggested that the Neoproterozoic radiation of eukaryotic phytoplankton (Brocks, 2018; Brocks et al., 2017; Zumberge et al., 2018), possibly spurred by increased eukaryovory (Cohen et al., 2011; Lenton and Daines, 2018; Porter, 2011), fundamentally transformed the biological carbon pump. Due to their greater cell size, it has been argued that emerging eukaryotic phytoplankton would have increased rates of

POC (particulate organic carbon) settling and thus export productivity (e.g., Butterfield, 2009; Lenton et al., 2014). Increased rates of export productivity, in turn, have been inferred to have enhanced water-column clarity and decreased water-column respiration, as well as increasing the efficiency of organic carbon burial, thus mediating both ocean and atmospheric oxygenation and fostering the emergence of increasingly complex, animal-rich benthic ecosystems (e.g., Butterfield, 2011). An assumption underlying this argument is that oxygenation, in the case of the Neoproterozoic ocean-atmosphere system, depends on eukaryotes as top-down levers on the marine carbon cycle. A question that has received less attention, however, is whether this is indeed a unique solution, as has been argued, to the question of what factor(s) drove oxygenation (Butterfield, 2009; Lenton et al., 2014). In other words, is eukaryotic life (or comparably complex modes of life) an essential prerequisite for achieving a well-oxygenated Earth system state?

As outlined above, geochemical and sedimentological archives indicate that the Paleoproterozoic was characterized by a pronounced interval of elevated oxygenation—likely equal in magnitude to that of the Neoproterozoic—which, although eventually followed by a decline in oxygen levels (Poulton et al., 2021), may have extended over hundreds of millions of years. Robust paleontological, geochemical, or molecular clock evidence, however, for a eukaryotic presence prior to the GOE is conspicuously absent. Sterane biomarkers—fossilized lipids involved in membrane regulation in eukaryotic organisms—detected in samples of the Neoproterozoic Fortescue and Hammersley groups of the Pilbara Craton of Western Australia were previously cited as possible evidence for eukaryotes (Brocks et al., 1999), but these have since been ruled out as contaminants (Rasmussen et al., 2008). Consistent with this challenge, recent efforts, employing more stringent sampling protocols, have failed to reproduce any signal for a eukaryotic contribution to the syngenetic organic contents of these rocks (French et al., 2015). It therefore seems improbable that the emergence of eukaryotes played a role in the onset of Paleoproterozoic oxygenation. However, the broader question of whether the GOE may have paved the way for the development of greater biological complexity, including the emergence of multicellular and eukaryotic life, has been a subject of contention.

5.1. Insights from fossil records

Identification of early eukaryotes in the body-fossil record has not proven straightforward, nor have these efforts been without controversy. There have been multiple claims for the rise of biological complexity and multicellularity during the Lomagundi associated with the creation of oxygenated shallow marine environments. Enigmatic, centimeter-scale pyritized structures preserved in the 2.1 Ga Francevillian Series B Formation of Gabon have been cited as possible evidence of complex, eukaryote-grade organisms (Fig. 5) (El Albani et al., 2010; El Albani et al., 2014; El Albani et al., 2019). Some of these structures have been interpreted as possible colonial eukaryotes (or organisms of a similar level of morphological and ecological complexity) on the basis of their large size, repeated and complex morphologies, and sulfur isotopic ($\delta^{34}\text{S}$) signatures (El Albani et al., 2010; El Albani et al., 2014). More recently, the same unit has yielded pyritized string-like structures that have been interpreted as mucus trails produced by slime mold-like organisms (El Albani et al., 2019). This suite of structures has been invoked as evidence that complex organisms emerged and explored a diverse range of morphologies and ecological strategies in the ephemerally but generally highly oxygenated world of the syn- and post-GOE Paleoproterozoic, and that mobile and infaunal multicellular organisms preceded the oldest previously documented occurrences of mobile and burrowing animals by over 1.5 billion years (El Albani et al., 2019). However, the biogenicity of the Francevillian structures has proven controversial (e.g., Knoll, 2011). Many of the most salient features associated with these structures may be equally consistent with an early diagenetic origin, such as pyrite suns, abiogenic concretions (Anderson

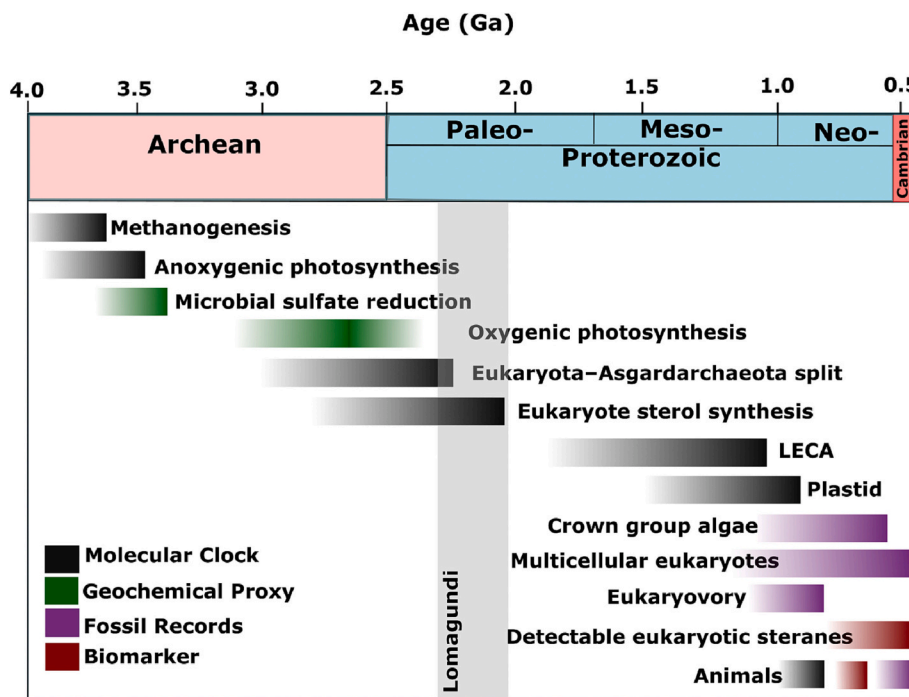


Fig. 5. Major events in the evolution of eukaryotic life on Earth. Green bars correspond to the emergence of important metabolic pathways based on geochemical proxies. Black bars denote major biological events inferred from molecular clock analyses. Purple and red bars refer to the information provided by the body and trace fossil records and biomarker records, respectively. The lengths of bars denote uncertainties in timing; ranges circumscribe estimates based on molecular clock analyses, geologic and geochemical evidence, and fossil records. Emerging evidence points toward ecological expansion of eukaryotic and animal life during the Mesoproterozoic–Neoproterozoic and Neoproterozoic, respectively, long after the Lomagundi, despite the considerable duration of well-oxygenated conditions at Earth's surface during the Lomagundi. Data on the timing of these events and innovations have been compiled from previous studies (Berney and Pawłowski, 2006; Betts et al., 2018; El Albani et al., 2019; Eme et al., 2014; Knoll and Nowak, 2017; Loran et al., 2019; Mills et al., 2022; Parfrey et al., 2011; Shih and Matzke, 2013).

et al., 2016), and syneresis cracks (cf. McMahon et al., 2017). The structures interpreted as possible slime mold analogs, in particular, occur along a continuum of highly variable morphologies, including variable sinuosity, diameter, and orientation, as well as pygmatoidal folding. This variability has been invoked as evidence in favor of a slime-mold-like organism. However, by this logic, a wide range of irregular features could be interpreted in this manner and, importantly, the features attributed to these structures by El Albani et al. (2014, 2019) are also classically associated with syneresis cracks (cf. McMahon et al., 2017). In light of their stratigraphic age, unusual morphology, and the relative rarity of these features, a eukaryote affinity for these features—or affinity with analogously complex multicellular organisms—remains uncertain. Similarly, paired sandstone ridges, described from the Stirling Range Formation (potentially as old as 2.0 Ga) of Western Australia, have been interpreted as mucus trails formed by motile, worm-like animals (cf. Rasmussen et al., 2002). However, a mucus trail origin for these structures has been disputed on both morphological and taphonomic grounds, in particular on the basis of their irregularity, high relief, and convex preservation on sandstone bed bases (e.g., Morris, 2002). Distinguishing between biogenic and abiogenic features of Paleoproterozoic age, as well as between syngenetic and later-stage processes, can be extremely challenging. As such, the Precambrian record is rife with structures that have been mistakenly interpreted in this manner (Seilacher, 2007). It is therefore reasonable to argue that putative records of eukaryotes or multicellularity during the Lomagundi currently fail to pass the stringent criteria for these structures to be viewed as bona fide fossils (cf. Seilacher, 2007).

The oldest potentially eukaryotic microfossils occur in the latest Paleoproterozoic Changzhongou Formation (ca. 1.8 Ga) and Chuanlinggou Formation (ca. 1.7 Ga) of North China (Lamb et al., 2009; Miao et al., 2019; Peng et al., 2009). These acritarchs (organic-walled microfossils), although of simple leiospheric morphology, range up to 250 μm in diameter, contain medial splits that may record encystment and may also be characterized by complex wall structure (Lamb et al., 2009; Miao et al., 2019; Peng et al., 2009). However, identification of these fossils as eukaryotic is tentative, and a non-eukaryote stem-group affinity cannot be ruled out. The oldest microfossils to which a eukaryotic affinity can confidently be assigned—forms such as *Shuiyousphaeridium*,

Tappania, *Satka*, and *Valeria*, characterized by morphological complexity, large size, and encystment structures (Fig. 5) (Javaux et al., 2004)—occur in the latest Paleoproterozoic–early Mesoproterozoic (ca. 1.8–1.6 Ga) Ruyang Group of China (Pang et al., 2015; Zhao, 2009) and the Mesoproterozoic (ca. 1.5 Ga) Roper Group of Australia (Javaux et al., 2004). Macroscopic fossils of potentially eukaryotic affinity, such as *Grypania* and *Horodyskia*, also occur in Mesoproterozoic successions of North America, China, and Western Australia (e.g., Grey and Williams, 1990; Javaux and Lepot, 2018; Knoll et al., 2006).

5.2. Insights from molecular clocks

Currently, molecular clock estimates suggest a story generally consistent with the microfossil record, with no evidence for eukaryotes during the Lomagundi interval or before ca. 1.8 Ga, more specifically (Berney and Pawłowski, 2006; Betts et al., 2018; Parfrey et al., 2011). Recent age estimates for divergence from the first eukaryotic common ancestor (FECA, e.g., the divergence between Archaea and Eukarya) range between 3.0 and 2.3 Ga, while those for the last eukaryotic common ancestor (LECA) range between 1.9 and 1.0 Ga (Fig. 5) (Berney and Pawłowski, 2006; Betts et al., 2018; Eme et al., 2014; Mills et al., 2022; Porter, 2020). The origin of total-group Alphaproteobacteria, within which the free-living ancestor of the mitochondrion is inferred to have diverged (and the possession of which is widely considered to be ancestral to crown-group eukaryotes), has been estimated to fall between 2.0 and 1.2 Ga (Berney and Pawłowski, 2006; Betts et al., 2018; Mills et al., 2022). Within these uncertainties, it remains possible that the eukaryotic stem-lineage (post-FECA) established its relationship with the free-living alphaproteobacterial ancestor of mitochondria well into the Proterozoic (no later than 1.2 Ga), potentially a billion years after both the GOE and the Lomagundi. In any case, all currently available fossil and molecular clock evidence indicate that eukaryotes emerged well after the Lomagundi, which—given multiple lines of evidence for well-oxygenated marine and atmospheric conditions during the Lomagundi—strongly suggests that a world without eukaryotes or animals would not necessarily remain trapped in a low-oxygen state and that an extended interval of high oxygen would not necessarily have triggered their emergence.

6. Did Lomagundi oxygenation set the stage for the appearance and diversification of complex life?

An updated view of the biotic and geochemical landscape of the Lomagundi interval suggests that, in contrast to some traditional views, more than 100 million years of pervasive oxygenation did not foster eukaryogenesis (Mänd et al., 2022). In the original formulation of Serial Endosymbiotic Theory (SET), Lynn Margulis (then Lynn Sagan) described eukaryotes, and more specifically mitochondria, as “fundamentally aerobic” (Sagan, 1967). To constrain when eukaryotes first evolved in Earth’s history, Margulis used Preston Cloud’s, 1965 estimate of 1.2 Ga for when “oxygen first began to be available in relatively large quantities” in the atmosphere (Cloud, 1965). In other words, Margulis explicitly tied the origin of mitochondria to Earth’s earliest oxygenation (as it was then understood), arguing that the ingestion of a fundamentally aerobic symbiont (the ancestral mitochondrion) by an anaerobic host was directly driven by survival in a newly oxygenated Earth system (Sagan, 1967). Fifty years later, the GOE is still suggested to have “facilitated the emergence of eukaryotes” (e.g., Knoll and Nowak, 2017).

Perhaps some of the most striking findings subsequent to SET were the discoveries of hydrogenosomes (anaerobic, H_2 - and ATP-producing organelles) and mitosomes (reduced forms of hydrogenosomes uninvolvement in ATP production) and their now agreed-upon common ancestry with mitochondria (Lindwiark and Muller, 1973; Martin, 2017; Müller et al., 2012). The recognition that LECA possessed mitochondria, that no primitively amitochondriate eukaryotes have ever been described, and that amitochondriate eukaryotes (those that today possess hydrogenosomes and mitosomes) appear to be polyphyletic and found across the eukaryotic tree all challenge early views that eukaryotic anaerobes never possessed mitochondria and that they all diverged prior to the acquisition of mitochondria during the GOE, as originally predicted by SET (e.g., Embley and Martin, 2006; Martin, 2017). The polyphyletic nature of amitochondrial eukaryotes implies multiple independent transitions to anaerobic lifestyles, but this would require multiple lateral transfers of bacterial genes involved in anaerobic metabolisms (Stairs et al., 2015). Another perhaps more likely possibility is that LECA, or at least the ancestral mitochondrion, was a facultative aerobe and that the apparent phylogenetic intermingling of aerobic and anaerobic eukaryotic lineages instead represents the differential loss of metabolic pathways across the eukaryotic tree (Martin and Müller, 1998; Müller et al., 2012), with little to no prokaryote-to-eukaryote or eukaryote-to-eukaryote lateral gene transfer (Ku et al., 2015; Ku and Martin, 2016; Tria et al., 2021), resulting in a limited and conserved subset of genes involved in anaerobic energy metabolism in eukaryotes (Müller et al., 2012).

Even if the evolution of hydrogenosomes ultimately involved the lateral transfer of bacterial genes (Spang et al., 2019), it remains possible that the original metabolic coupling between the host and symbiont was strictly anaerobic and could have predated the GOE (Martin and Müller, 1998; Moreira and López-García, 1998). Critically, this would decouple the earliest stages of eukaryogenesis from the oxygenation of Earth’s surface environment, *contra* SET, which argues that oxygen utilization in the wake of biospheric oxygenation was the foundation of the symbiont-host relationship. Most recently, proponents of the E^3 model (Entangle-Engulf-Enslave) of eukaryogenesis have suggested that the host—an anaerobic and fermenting archaeon dependent on syntrophy for amino acid degradation—would have depended on H_2 -scavenging methanogenic partners for growth prior to the GOE (Imachi et al., 2019; Mills et al., 2022). After the GOE, under the selective regime of a more heterogeneous redox landscape, the host cell would have become dependent on sulfate-reducing bacteria (SRB) for H_2 scavenging, as well as on the free-living ancestor of the mitochondrion (a facultative aerobe) for O_2 -scavenging and metabolite exchange, at an oxic-anoxic interface (Imachi et al., 2019). However, this three-partner association would also have been encouraged under anoxia, where the SRB and the ancestral mitochondrion would have interacted via H_2

scavenging and anaerobic H_2 -producing organotrophy, respectively. There are multiple viable models for the origin of both mitochondria and eukaryotes—but critically, eukaryogenesis need not be linked to the GOE or the emergence of well-oxygenated conditions.

Eukaryotes appear to have increased in diversity and ecological complexity beginning in the latest Mesoproterozoic and early Tonian (e.g., Loron and Moczyłowska, 2017; Loron et al., 2019; Zumberge et al., 2018, 2020) and continued to radiate and increase in ecological importance through the Neoproterozoic and early Phanerozoic (Brocks, 2018; Knoll et al., 2006). This interval also witnessed major climatic perturbations (the Snowball Earth glacial) and likely both stepwise and progressive increases (and potential decreases) in oxygen concentrations (Lyons et al., 2014, 2021; Och and Shields-Zhou, 2012; Shields-Zhou and Och, 2011; Wallace et al., 2017). The history of this interval is still being pieced together but, as has been discussed extensively elsewhere, as well as in the preceding sections, it is plausible that some of these biotic and environmental changes are intimately linked. The oldest sterane biomarkers, recovered from kerogen and bitumen extracted from Tonian and Cryogenian strata, record the initiation of a measurable eukaryotic (green- and red-algal) contribution to primary production during this same interval (Brocks, 2018; Zumberge et al., 2020). The nearly billion-year gap between the late Paleoproterozoic–Mesoproterozoic emergence of bona fide eukaryotic microfossils and the appearance of eukaryote-produced steranes in the Neoproterozoic highlights one of the most puzzling enigmas in the emergence of complex life. One possible explanation lies in the potentially stem-eukaryote affiliation of many (perhaps the majority) of upper Paleoproterozoic and Mesoproterozoic fossils that have been attributed to eukaryotes, particularly if stem-eukaryotes did not produce sterols (e.g., Porter, 2020; Porter et al., 2018). If LECA did not in fact appear until the late Mesoproterozoic, this apparent temporal discrepancy would be partially ameliorated.

Moreover, if the acquisition of mitochondria, and thus the capacity for aerobic respiration, was a derived feature for crown-group Eukarya, this relationship, combined with geochemical evidence for intervals of widespread anoxia in the shallow Mesoproterozoic oceans (Lyons et al., 2014; Tang et al., 2016), might indicate that many stem-group eukaryotes were facultative or even obligatory anaerobes (Porter et al., 2018). As sterol synthesis likely requires both mitochondria and oxygen (e.g., Desmond and Gribaldo, 2009; Porter et al., 2018), an anaerobic life mode for pre-LECA stem-group eukaryotes (and a facultatively or secondarily obligatory anaerobic life mode for early members of the crown group) may further explain the gap between eukaryotic origins without an associated sterane record and the proliferation of algal phytoplankton recorded by Neoproterozoic steranes. However, molecular clock evidence for the early emergence of the eukaryotic capacity to produce sterols casts some doubt on this framework (Gold et al., 2017). Moreover, body fossils of multicellular, crown-group algae—which would certainly have required appreciable oxygen levels and practiced sterol synthesis—have been documented from multiple upper Mesoproterozoic–lower Tonian successions (e.g., Butterfield, 2000; Tang et al., 2020). Therefore, it is likely that, at least in local oxygenated benthic microenvironments, eukaryotic algae were present by the late Mesoproterozoic and early Neoproterozoic, but perhaps insufficiently abundant to produce a measurable sterane contribution to bulk sedimentary organic matter (e.g., Lyons et al., 2021). Ultimately, these observations are also consistent with the idea that even if the high oxygen levels of the Lomagundi facilitated the development of the biotic novelties integral to eukaryotic life, there was an extended (potentially up to a billion-year) macroevolutionary lag between the development of eukaryotic novelties and their ecologically and environmentally widespread implementation as biotic innovations (cf. Erwin, 2015). The ecological impact of eukaryotes may therefore have been relatively muted prior to the late Neoproterozoic.

In sum, coupled paleontological, molecular, and geochemical records strongly suggest that oxygenation during the Lomagundi was

neither induced by nor the cause of notable increases in biological complexity and appears to have been temporally decoupled from extensive diversification and ecological expansion of eukaryotes. Instead, Lomagundi oxygenation must have occurred in an Earth system where primary production was bacterial and biological complexity was limited to bacterial and archaeal cells, as well as their intercellular interactions. By extension, this possibility implies both that a world lacking eukaryotes would not necessarily remain trapped in a low-oxygen state and that well-oxygenated atmospheres need not trigger biological complexity beyond simple cells and their interactions.

7. Drivers of Lomagundi oxygenation

If biological innovations in eukaryotes are an unlikely driver of oxygenation for the Lomagundi, this begs the question of what caused ocean-atmosphere oxygenation during this period. One possibility is that oxidation of Archean crust rich in siderite and sulfides promoted enhanced phosphorus and sulfate fluxes to the oceans (Bachan and Kump, 2015; Bekker et al., 2016; Bekker and Holland, 2012; Konhauser et al., 2011). Given that phosphorus is generally agreed to be the nutrient limiting the productivity of the marine biosphere on geologic timescales (Reinhard et al., 2017; Tyrrell, 1999), enhanced phosphorus fluxes would be predicted to lead to more organic carbon burial and thus oxygenation. Further, oxygenation and ingrowth of the sulfate reservoir would have dramatically decreased iron fluxes to the oceans from hydrothermal systems (Kump and Seyfried, 2005), which is critical since P/Fe ratios are thought to play a key role in regulating biospheric oxygen fluxes (Jones et al., 2015; Ozaki et al., 2019). Competition for phosphorus between oxygenic and anoxygenic photosynthesis provides a means to restrict oxygen production rates in anoxic oceans. In this framework, the duration of the Lomagundi would ultimately be limited to the time span needed for the continental weatherable shell to transition from being rich in reduced mineral species (and associated with increased liberation of phosphorus) to being rich in oxidized mineral species. Under this framework, similar processes could, in theory, have promoted oxygenation during the Neoproterozoic—after a prolonged interval of pervasive anoxia in the deep ocean and low-oxygen conditions in the shallow ocean (Arnold et al., 2004; Planavsky et al., 2011, 2014b; Shen et al., 2003; Tang et al., 2016). However, this possibility leaves open the question of why the elevated oxygen levels that characterized the Lomagundi did not persist beyond several hundreds of millions of years—in spite of the stabilizing feedbacks predicted to regulate a well-oxygenated ocean-atmosphere system (e.g., Laakso and Schrag, 2017)—while the Earth system appears to have remained stable and mostly well-oxygenated following the NOE.

8. Conclusions

We argue that taking a broad look at the Precambrian permits a balanced consideration of the extent to which environmental and biotic change have been linked through Earth's history. Archean and Proterozoic records provide clear examples of how even profoundly important biotic novelties (cf. Erwin, 2015)—such as oxygenic photosynthesis or the emergence of eukaryotes—may be followed by appreciable macroevolutionary lags and not immediately drive fundamental environmental change or ecological innovation. For example, Paleoproterozoic archives indicative of an extended interval of stable oxygenation associated with the Lomagundi suggest that the emergence of biological complexity (e.g., eukaryogenesis) is not a prerequisite for large-scale oxygenation and, conversely, that oxygenation need not immediately foster associated increases in biological complexity. In contrast, Mesoproterozoic and Neoproterozoic records suggest that environmental conditions can reshape ecosystem structure and thus facilitate the 'long-fuse' development of major biological and ecological innovations. Therefore, our current picture of Earth's history does not give the simple message once envisioned regarding the links between oxygenation and

the rise of complexity (Cloud, 1965; Knoll and Nowak, 2017; Sagan, 1967). Instead, the emerging view is that similar Earth system states have hosted markedly different biospheres and biotic-environmental relationships, for intervals lasting hundreds of millions of years, over our planet's history.

Declaration of Competing Interest

The authors declare no conflict of interest.
Mojtaba Fakhraee (on behalf of co-authors)

Data availability

No new data were used for the research described in the article.

Acknowledgments

This study benefited from discussion with A. Bauer, D. Mills, A. Rooney and was supported by a National Aeronautics and Space Administration Interdisciplinary Consortia for Astrobiology Research grant (NNA15BB03A) to T.W.L., C.T.R., and N.J.P. We thank A. Negri, S. Porter and an anonymous reviewer for critical feedback that improved this manuscript.

References

- Albut, G., Kamber, B.S., Briske, A., Beukes, N.J., Smith, A.J.B., Schoenberg, R., 2019. Modern weathering in outcrop samples versus ancient paleoredox information in drill core samples from a Mesoproterozoic marine oxygen oasis in Pongola Supergroup, South Africa. *Geochim. Cosmochim. Acta* 265, 330–353. <https://doi.org/10.1016/j.gca.2019.09.001>.
- Alcott, L.J., Mills, B.J.W., Poulton, S.W., 2019. Stepwise Earth oxygenation is an inherent property of global biogeochemical cycling. *Science* 366, 1333–1337. <https://doi.org/10.1126/science.aax6459>.
- Anderson, R.P., Tarhan, L.G., Cummings, K.E., Planavsky, N.J., Bjørnerud, M., 2016. Macroscopic Structures in the 1.1 Ga Continental Copper Harbor Formation: Concretions or Fossils? *Palaios* 31, 327–338. <https://doi.org/10.2110/PAL0.2016.013>.
- Arnold, G.L., Anbar, A.D., Barling, J., Lyons, T.W., 2004. Molybdenum Isotope evidence for Widespread Anoxia in Mid-Proterozoic Oceans. *Science* 304, 87–90. <https://doi.org/10.1126/science.1091785>.
- Avila, D., Cardenas, R., Martin, O., 2013. In: On the Photosynthetic Potential in the Very Early Archean Oceans, pp. 67–75. <https://doi.org/10.1007/s11084-012-9322-1>.
- Awramik, S.M., 1992. The oldest records of photosynthesis. *Photosynth. Res.* <https://doi.org/10.1007/BF00039172>.
- Bachan, A., Kump, L.R., 2015. The rise of oxygen and siderite oxidation during the Lomagundi event. *Proc. Natl. Acad. Sci. U. S. A.* 112, 6562–6567. <https://doi.org/10.1073/pnas.1422319112>.
- Bao, H., Lyons, J.R., Zhou, C., 2008. Triple oxygen isotope evidence for elevated CO₂ levels after a Neoproterozoic glaciation. *Nature* 453, 504–506. <https://doi.org/10.1038/nature06959>.
- Battistuzzi, F.U., Feijao, A., Hedges, S.B., 2004. A genomic timescale of prokaryote evolution: insights into the origin of methanogenesis, phototrophy, and the colonization of land, 14, 1–14. <https://doi.org/10.1186/1471-2148-4-44>.
- Bekker, A., 2019. Encyclopedia of Astrobiology. *Encyclop. Astrobiol.* 1–9 <https://doi.org/10.1007/978-3-642-27833-4>.
- Bekker, A., Holland, H.D., 2012. Oxygen overshoot and recovery during the early Paleoproterozoic. *Earth Planet. Sci. Lett.* 317–318, 295–304. <https://doi.org/10.1016/j.epsl.2011.12.012>.
- Bekker, A., Holland, H.D., Wang, P.-L., Rumble, D., Stein, H.J., Hannah, J.L., Coetzee, L., Beukes, N.J., 2004. Dating the rise of Oxygen. *Nature* 427, 117–120. <https://doi.org/10.1038/nature02260>.
- Bekker, A., Kaufman, A.J., Karhu, J.A., Beukes, N.J., Swart, Q.D., Coetzee, L.L., Eriksson, K.A., 2001. Chemostratigraphy of the Paleoproterozoic Duitschland Formation, South Africa: Implications for coupled climate change and carbon cycling. *Am. J. Sci.* 301, 261–285. <https://doi.org/10.2475/aj.sci.301.3.261>.
- Bekker, A., Krapez, B., Müller, S.G., Karhu, J.A., 2016. A short-term, post-lomagundi positive C isotope excursion at C. 2.03 Ga recorded by the woolly dolomite, Western Australia. *J. Geol. Soc. Lond.* 173, 689–700. <https://doi.org/10.1144/jgs2015-152>.
- Bekker, A., Slack, J.F., Planavsky, N., Krapez, B., Hofmann, A., Konhauser, K.O., Rouxel, O.J., 2010. Iron Formation: the Sedimentary product of a complex Interplay among Mantle, Tectonic, Oceanic, and Biospheric Processes. *Econ. Geol.* 105, 467–508. <https://doi.org/10.2113/GSECONGEO.105.3.467>.
- Berney, C., Pawlowski, J., 2006. A molecular time-scale for eukaryote evolution recalibrated with the continuous microfossil record. *Proc. R. Soc. B Biol. Sci.* 273, 1867–1872. <https://doi.org/10.1098/rspb.2006.3537>.
- Betts, H.C., Puttick, M.N., Clark, J.W., Williams, T.A., Donoghue, P.C.J., Pisani, D., 2018. Integrated genomic and fossil evidence illuminates life's early evolution and

- eukaryote origin. *Nat. Ecol. Evol.* 2, 1556–1562. <https://doi.org/10.1038/s41559-018-0644-x>.
- Beukes, N.J., Dorland, H., Gutzmer, J., Nedachi, M., Ohmoto, H., 2002. Tropical laterites, life on land, and the history of atmospheric oxygen in the Paleoproterozoic. *Geology* 30, 491–494. [https://doi.org/10.1130/0091-7613\(2002\)030<0491:TLOLA>2.0.CO;2](https://doi.org/10.1130/0091-7613(2002)030<0491:TLOLA>2.0.CO;2).
- Blättler, C.L., Claire, M.W., Prave, A.R., Kirsimäe, K., Higgins, J.A., Medvedev, P.V., Romashkin, A.E., Rychanchik, D.V., Zerkle, A.L., Paiste, K., Kreitsmann, T., Millar, I. L., Hayles, J.A., Bao, H., Turchyn, A.V., Warke, M.R., Lepland, A., 2018. Two-billion-year-old evaporites capture Earth's great oxidation. Downloaded from. *Science*.
- Boden, J.S., Konhauser, K.O., Robbins, L.J., Sánchez-Baracaldo, P., 2021. Timing the evolution of antioxidant enzymes in cyanobacteria. *Nat. Commun.* 12 (1), 1–12. <https://doi.org/10.1038/s41467-021-24396-y>.
- Brocks, J.J., 2018. The transition from a cyanobacterial to algal world and the emergence of animals. *Emerg. Top. Life Sci.* 2, 181–190. <https://doi.org/10.1042/etls20180039>.
- Brocks, J.J., Logan, G.A., Buick, R., Summons, R.E., 1999. Archean molecular fossils and the early rise of eukaryotes. *Science* 285, 1033–1036. <https://doi.org/10.1126/science.285.5430.1033>.
- Brocks, J.J.M., Jarrett, A.J., Sirantoin, E., Hallmann, C., Hoshino, Y., Liyanage, T., 2017. The rise of algae in Cryogenian oceans and the emergence of animals. *Nat. Publ. Group* 548. <https://doi.org/10.1038/nature23457>.
- Butterfield, N.J., 2011. Animals and the invention of the Phanerozoic Earth system. *Trends Ecol. Evol.* 26, 81–87. <https://doi.org/10.1016/j.tree.2010.11.012>.
- Butterfield, N.J., 2009. Oxygen, animals and oceanic ventilation: an alternative view. *Geobiology* 7, 1–7. <https://doi.org/10.1111/j.1472-4669.2009.00188.x>.
- Butterfield, N.J., 2000. *Bangiomorpha pubescens* n. Gen., n. Sp.: implications for the evolution of sex, multicellularity, and the Mesoproterozoic/Neoproterozoic radiation of eukaryotes. *Paleobiology* 26, 386–404. [https://doi.org/10.1666/0094-8373\(2000\)026<0386:bpngns>2.0.co;2](https://doi.org/10.1666/0094-8373(2000)026<0386:bpngns>2.0.co;2).
- Butterfield, N.J., 1997. Planktonic ecology and the Proterozoic-Phanerozoic transition. *Paleobiology* 23, 247–262. <https://doi.org/10.1017/S009483730001681X>.
- Campbell, I.H., Allen, C.M., 2008. Formation of supercontinents linked to increases in atmospheric oxygen. *Nat. Geosci.* 1, 554–558. <https://doi.org/10.1038/ngeo259>.
- Canfield, D.E., 2021. Carbon cycle evolution before and after the Great Oxidation of the atmosphere. *Am. J. Sci.* 321, 297–331. <https://doi.org/10.2475/03.2021.01>.
- Canfield, D.E., 2005. The early history of atmospheric oxygen: Homage to Robert M. Garrels. *Annu. Rev. Earth Planet. Sci.* 33, 1–36. <https://doi.org/10.1146/annurev.earth.33.092203.122711>.
- Canfield, D.E., Farquhar, J., 2009. Animal evolution, bioturbation, and the sulfate concentration of the oceans. *Proc. Natl. Acad. Sci. U. S. A.* 106, 8123–8127. <https://doi.org/10.1073/PNAS.0902037106>.
- Canfield, D.E., Glazer, A.N., Falkowski, P.G., 2010. The Evolution and Future of Earth's Nitrogen Cycle. *Science* 330, 192–196. <https://doi.org/10.1126/SCIENCE.1186120>.
- Canfield, D.E., Poulton, S.W., Knoll, A.H., Narbonne, G.M., Ross, G., Goldberg, T., Strauss, H., 2008. Ferruginous conditions dominated later neoproterozoic deep-water chemistry. *Science* 321, 949–952. <https://doi.org/10.1126/science.1154499>.
- Canfield, D.E., Poulton, S.W., Narbonne, G.M., 2007. Late-Neoproterozoic deep-ocean oxygenation and the rise of animal life. *Science* 315, 92–95. <https://doi.org/10.1126/science.1135013>.
- Cardona, T., Sánchez-Baracaldo, P., Rutherford, A.W., Larkum, A.W., 2019. Early Archean origin of Photosystem II. *Geobiology* 17, 127–150. <https://doi.org/10.1111/GBI.12322>.
- Catling, D.C., Glein, C.R., Zahnle, K.J., McKay, C.P., 2005. Why O₂ is required by complex life on habitable planets and the concept of planetary "Oxygenation time". *Astrobiology*. <https://doi.org/10.1089/ast.2005.5.415>.
- Chi Fru, E., Rodra-Guez, N.P., Partin, C.A., Lalonde, S.V., Andersson, P., Weiss, D.J., Albani, A., Rodushkin, I., Konhauser, K.O., 2016. Cu isotopes in marine black shales record the Great Oxidation Event. *Proc. Natl. Acad. Sci. USA* 113, 4941–4946. https://doi.org/10.1073/PNAS.1523544113/SUPPL_FILE/PNAS.1523544113.SD02.XLSX.
- Chi Fru, E., Somogyi, A., Albani, A., Medjoubi, K., Aubineau, J., Robbins, L.J., Lalonde, S. V., Konhauser, K.O., 2019. The rise of oxygen-driven arsenic cycling at ca. 2.48 Ga. *Geology* 47, 243–246. <https://doi.org/10.1130/G45676.1>.
- Cloud, P.E., 1965. Significance of the gunflint (precambrian) microflora. *Science* 149, 27–35. <https://doi.org/10.1126/science.148.3666.27>.
- Cohen, P.A., Schopf, J.W., Butterfield, N.J., Kudryavtsev, A.B., Macdonald, F.A., 2011. Phosphate biomineralization in mid-neoproterozoic protists. *Geology* 39, 539–542. <https://doi.org/10.1130/G31833.1>.
- Cole, D.B., Mills, D.B., Erwin, D.H., Sperling, E.A., Porter, S.M., Reinhard, C.T., Planavsky, N.J., 2020. On the co-evolution of surface oxygen levels and animals. *Geobiology* 18, 260–281. <https://doi.org/10.1111/GBI.12382>.
- Cole, D.B., Reinhard, C.T., Wang, X., Gueguen, B., Halverson, G.P., Gibson, T., Hodgskiss, M.S.W., Ryan McKenzie, N., Lyons, T.W., Planavsky, N.J., 2016. A shale-hosted Cr isotope record of low atmospheric oxygen during the Proterozoic. *Geology* 44, 555–558. <https://doi.org/10.1130/G37787.1>.
- Colwyn, D.A., Sheldon, N.D., Maynard, J.B., Gaines, R., Hofmann, A., Wang, X., Gueguen, B., Asael, D., Reinhard, C.T., Planavsky, N.J., 2019. A paleosol record of the evolution of Cr redox cycling and evidence for an increase in atmospheric oxygen during the Neoproterozoic. *Geobiology* 17, 579–593. <https://doi.org/10.1111/gbi.12360>.
- Cox, G.M., Lyons, T.W., Mitchell, R.N., Hasterok, D., Gard, M., 2018. Linking the rise of atmospheric oxygen to growth in the continental phosphorus inventory. *Earth Planet. Sci. Lett.* 489, 28–36. <https://doi.org/10.1016/J.EPSL.2018.02.016>.
- Crockford, P.W., Hayles, J.A., Bao, H., Planavsky, N.J., Bekker, A., Fralick, P.W., Halverson, G.P., Bui, T.H., Peng, Y., Wing, B.A., 2018. Triple oxygen isotope evidence for limited mid-Proterozoic primary productivity. *Nature*. <https://doi.org/10.1038/s41586-018-0349-y>.
- Crockford, P.W., Kunzmann, M., Bekker, A., Hayles, J., Bao, H., Halverson, G.P., Peng, Y., Bui, T.H., Cox, G.M., Gibson, T.M., Wöhrle, S., Rainbird, R., Lepland, A., Swanson-Hysell, N.L., Master, S., Sreenivas, B., Whitezov, A., Krupnik, V., Wing, B. A., 2019. Claypool continued: Extending the isotopic record of sedimentary sulfate. *Chem. Geol.* <https://doi.org/10.1016/j.chemgeo.2019.02.030>.
- Crowe, S.A., Dossing, L.N., Beukes, N.J., Bau, M., Kruger, S.J., Frei, R., Canfield, D.E., 2013. Atmospheric oxygenation three billion years ago. *Nature*. <https://doi.org/10.1038/nature12426>.
- Crowe, S.A., Paris, G., Katsev, S., Jones, C.A., Kim, S.T., Zerkle, A.L., Nomosatryo, S., Fowle, D.A., Adkins, J.F., Sessions, A.L., Farquhar, J., Canfield, D.E., 2014. Sulfate was a trace constituent of Archean seawater. *Science* 346, 735–739. <https://doi.org/10.1126/science.1258966>.
- Czaja, A.D., Johnson, C.M., Roden, E.E., Beard, B.L., Voegelin, A.R., Nägler, T.F., Beukes, N.J., Wille, M., 2012. Evidence for free oxygen in the Neoproterozoic Ocean based on coupled iron-molybdenum isotope fractionation. *Geochim. Cosmochim. Acta* 86, 118–137. <https://doi.org/10.1016/j.gca.2012.03.007>.
- Daines, S.J., Mills, B.J.W., Lenton, T.M., 2017. Atmospheric oxygen regulation at low Proterozoic levels by incomplete oxidative weathering of sedimentary organic carbon. *Nat. Commun.* 8. <https://doi.org/10.1038/ncomms14379>.
- Desmond, E., Gribaldo, S., 2009. Phylogenomics of Sterol Synthesis: Insights into the Origin, Evolution, and Diversity of a Key Eukaryotic Feature. *Genome Biol. Evol.* 1, 364–381. <https://doi.org/10.1093/gbe/evp036>.
- Duncan, M.S., Dasgupta, R., 2017. Rise of Earth's atmospheric oxygen controlled by efficient subduction of organic carbon. *Nat. Geosci.* 10, 387–392. <https://doi.org/10.1038/ngeo2939>.
- El Albani, A., Bengtson, S., Canfield, D.E., Bekker, A., Macchiarelli, R., Mazurier, A., Hammarlund, E.U., Boulvais, P., Dupuy, J.J., Fontaine, C., Fürsich, F.T., Gauthier-Lafaye, F., Janvier, P., Javau, E., Ossa, F.O., Pierson-Wickmann, A.C., Riboulleau, A., Sardini, P., Vachard, D., Whitehouse, M., Meunier, A., 2010. Large colonial organisms with coordinated growth in oxygenated environments 2.1 Gyr ago. *Nature* 466, 100–104. <https://doi.org/10.1038/nature09166>.
- El Albani, A., Bengtson, S., Canfield, D.E., Riboulleau, A., Bard, C.R., Macchiarelli, R., Pemba, L.N., Hammarlund, E., Meunier, A., Moule, I.M., Benzerara, K., Bernard, S., Boulvais, P., Chaussidon, M., Cesari, C., Fontaine, C., Chi Fru, E., Ruiz, J.M.G., Gauthier-Lafaye, F., Mazurier, A., Pierson-Wickmann, A.C., Rouxel, O., Trentesaux, A., Vecoli, M., Versteegh, G.J.M., White, L., Whitehouse, M., Bekker, A., 2014. The 2.1 Ga old Francevillian biota: Biogenicity, taphonomy and biodiversity. *PLoS One* 9. <https://doi.org/10.1371/journal.pone.0099438>.
- El Albani, A., Gabriella Mangano, M., Buatois, L.A., Bengtson, S., Riboulleau, A., Bekker, A., Konhauser, K., Lyons, T., Rollion-Bard, C., Bankole, O., Baghekema, S.G. L., Meunier, A., Trentesaux, A., Mazurier, A., Aubineau, J., Laforest, C., Fontaine, C., Recourt, P., Chi Fru, E., Macchiarelli, R., Reynaud, J.Y., Gauthier-Lafaye, F., Canfield, D.E., 2019. Organism motility in an oxygenated shallow-marine environment 2.1 billion years ago. *Proc. Natl. Acad. Sci. U. S. A.* 116, 3431–3436. <https://doi.org/10.1073/pnas.1815721116>.
- Embley, T.M., Martin, W., 2006. Eukaryotic evolution, changes and challenges. *Nature*. <https://doi.org/10.1038/nature04546>.
- Eme, L., Sharpe, S.C., Brown, M.W., Roger, A.J., 2014. On the Age of Eukaryotes: evaluating evidence from Fossils and Molecular Clocks. *Cold Spring Harb. Perspect. Biol.* 6, a016139. <https://doi.org/10.1101/CSHPERSPECT.A016139>.
- Eriksson, P.G., Cheney, E.S., 1992. Evidence for the transition to an oxygen-rich atmosphere during the evolution of red beds in the lower proterozoic sequences of southern Africa. *Precambrian Res.* 54, 257–269. [https://doi.org/10.1016/0301-9268\(92\)90073-W](https://doi.org/10.1016/0301-9268(92)90073-W).
- Erwin, D.H., 2015. Novelty and innovation in the history of life. *Curr. Biol.* <https://doi.org/10.1016/j.cub.2015.08.019>.
- Fakhraee, M., Crowe, S.A., Katsev, S., 2018. Sedimentary sulfur isotopes and Neoproterozoic ocean oxygenation. *Sci. Adv.* 4. <https://doi.org/10.1126/sciadv.1701835>.
- Fakhraee, M., Hancisse, O., Canfield, D.E., Crowe, S.A., Katsev, S., 2019. Proterozoic seawater sulfate scarcity and the evolution of ocean-atmosphere chemistry. *Nat. Geosci.* 12, 375–380. <https://doi.org/10.1038/s41561-019-0351-5>.
- Fakhraee, M., Planavsky, N.J., Reinhard, C.T., 2020. The role of environmental factors in the long-term evolution of the marine biological pump. *Nat. Geosci.* 13, 812–816. <https://doi.org/10.1038/s41561-020-00660-6>.
- Farquhar, J., Bao, H., Thiemens, M., 2000. Atmospheric influence of Earth's earliest sulfur cycle. *Science* 289, 756–758. <https://doi.org/10.1126/science.289.5480.756>.
- Farquhar, J., Wing, B.A., 2003. Multiple sulfur isotopes and the evolution of the atmosphere. *Earth Planet. Sci. Lett.* [https://doi.org/10.1016/S0012-821X\(03\)00296-6](https://doi.org/10.1016/S0012-821X(03)00296-6).
- Fischer, W.W., Fike, D.A., Johnson, J.E., Raub, T.D., Guan, Y., Kirschvink, J.L., Eiler, J. M., 2014. SQUID-SIMS is a useful approach to uncover primary signals in the Archean sulfur cycle. *Proc. Natl. Acad. Sci. U. S. A.* 111, 5468–5473. <https://doi.org/10.1073/PNAS.1322577111>.
- Fischer, W.W., Hemp, J., Johnson, J.E., 2016. Evolution of Oxygenic Photosynthesis. *Annu. Rev. Earth Planet. Sci.* 44, 647–683. <https://doi.org/10.1146/annurev-earth-060313-054810>.
- Fournier, G.P., Moore, K.R., Rangel, L.T., Payette, J.G., Momper, L., Bosak, T., 2021. The Archean origin of oxygenic photosynthesis and extant cyanobacterial lineages. *Proc. R. Soc. B* 288. <https://doi.org/10.1098/RSPB.2021.0675>.
- Fralick, P., Planavsky, N., Burton, J., Jarvis, I., Addison, W.D., Barrett, T.J., Brumpton, G. R., 2017. Geochemistry of Paleoproterozoic Gunflint Formation carbonate:

- Implications for hydrosphere-atmosphere evolution. *Precambrian Res.* 290, 126–146. <https://doi.org/10.1016/j.precamres.2016.12.014>.
- Frei, R., Gaucher, C., Stolper, D., Canfield, D.E., 2013. Fluctuations in late Neoproterozoic atmospheric oxidation - Cr isotope chemostratigraphy and iron speciation of the late Ediacaran lower Arroyo del Soldado Group (Uruguay). *Gondwana Res.* 23, 797–811. <https://doi.org/10.1016/j.gr.2012.06.004>.
- French, K.L., Hallmann, C., Hope, J.M., Schoon, P.L., Zumberge, J.A., Hoshino, Y., Peters, C.A., George, S.C., Love, G.D., Brocks, J.J., Buick, R., Summons, R.E., 2015. Reappraisal of hydrocarbon biomarkers in Archean rocks. *Proc. Natl. Acad. Sci. U. S. A.* 112, 5915–5920. <https://doi.org/10.1073/pnas.1419563112>.
- Garvin, J., Buick, R., Anbar, A.D., Arnold, G.L., Kaufman, A.J., 2009. Isotopic evidence for an aerobic nitrogen cycle in the latest Archean. *Science* 323(323), 1045–1048. <https://doi.org/10.1126/science.1165675>.
- Geyman, E.C., Maloof, A.C., 2021. Facies control on carbonate $\delta^{13}\text{C}$ on the Great Bahama Bank. *Geology* 49, 1049–1054. <https://doi.org/10.1130/G48862.1>.
- Geyman, E.C., Maloof, A.C., 2019. A diurnal carbon engine explains 13 C-enriched carbonates without increasing the global production of oxygen. *Proc. Natl. Acad. Sci.* 201908783 <https://doi.org/10.1073/pnas.1908783116>. Royal Society.
- Gilleaudeau, G.J., Frei, R., Kaufman, A.J., Kah, L.C., Azmy, K., Bartley, J.K., Chernyavskiy, P., Knoll, A.H., 2016. Oxygenation of the mid-Proterozoic atmosphere: Clues from chromium isotopes in carbonates. *Geochem. Perspect. Lett.* 2, 178–187. <https://doi.org/10.7185/geochemlet.1618>.
- Gold, D.A., Caron, A., Fournier, G.P., Summons, R.E., 2017. Paleoproterozoic sterol biosynthesis and the rise of oxygen. *Nature* 543 (7645), 420–423. <https://doi.org/10.1038/nature21412>.
- Grey, K., Williams, I.R., 1990. Problematic bedding-plane markings from the Middle Proterozoic Manganese Subgroup, Bangemall Basin, Western Australia. *Precambrian Res.* 46, 307–327. [https://doi.org/10.1016/0301-9268\(90\)90018-L](https://doi.org/10.1016/0301-9268(90)90018-L).
- Gross, J., Bhattacharya, D., 2010. Uniting sex and eukaryote origins in an emerging oxygenic world. *Biol. Direct* 5, 1–20. <https://doi.org/10.1186/1745-6150-5-53/FIGURES/2>.
- Guilbaud, R., Poulton, S.W., Butterfield, N.J., Zhu, M., Shields-Zhou, G.A., 2015. A global transition to ferruginous conditions in the early Neoproterozoic oceans. *Nat. Geosci.* 8, 1–5. <https://doi.org/10.1038/NGEO2434>.
- Halevy, I., Peters, S.E., Fischer, W.W., 2012. Sulfate burial constraints on the Phanerozoic sulfur cycle. *Science* 337(337), 331–334. <https://doi.org/10.1126/science.1220224>.
- Hannah, J.L., Bekker, A., Stein, H.J., Markey, R.J., Holland, H.D., 2004. Primitive Os and ^{231}Re Ma age for marine shale: Implications for Paleoproterozoic glacial events and the rise of atmospheric oxygen. *Earth Planet. Sci. Lett.* 225, 43–52. <https://doi.org/10.1016/j.epsl.2004.06.013>.
- Hao, W., Mänd, K., Li, Y., Alessi, D.S., Somelar, P., Moussavou, M., Romashkin, A.E., Lepand, A., Kirsimäe, K., Planavsky, N.J., Konhauser, K.O., 2021. The kaolinite shuttle links the Great Oxidation and Lomagundi events. *Nat. Commun.* 12 (1), 1–6. <https://doi.org/10.1038/s41467-021-23304-8>.
- Hardisty, D.S., Lu, Z., Bekker, A., Diamond, C.W., Gill, B.C., Jiang, G., Kah, L.C., Knoll, A.H., Loyd, S.J., Osburn, M.R., Planavsky, N.J., Wang, C., Zhou, X., Lyons, T.W., 2017. Perspectives on Proterozoic surface ocean redox from iodine contents in ancient and recent carbonate. *Earth Planet. Sci. Lett.* 463, 159–170. <https://doi.org/10.1016/j.epsl.2017.01.032>.
- Hardisty, D.S., Lu, Z., Planavsky, N.J., Bekker, A., Philippot, P., Zhou, X., Lyons, T.W., 2014. An iodine record of Paleoproterozoic surface ocean oxygenation. *Geology* 42, 619–622. <https://doi.org/10.1130/G35439.1>.
- Hayles, J.A., Cao, X., Bao, H., 2016. The statistical mechanical basis of the triple isotope fractionation relationship. *Geochem. Perspect. Lett.* 1–11 <https://doi.org/10.7185/geochemlet.1701>.
- Hodgskiss, M.S.W., Crockford, P.W., Peng, Y., Wing, B.A., Horner, T.J., 2019. A productivity collapse to end Earth's Great Oxidation. *Proc. Natl. Acad. Sci.* 201900325 <https://doi.org/10.1073/pnas.1900325116>.
- Hodgskiss, M.S.W., Crockford, P.W., Turchyn, A., 2023. Deconstructing the Lomagundi-Jatuli Carbon Isotope Excursion. *Ann. Rev. Earth Planet. Sci.* 51 <https://doi.org/10.1146/ANNUREV-EARTH-031621-071250>.
- Holland, H.D., 2006. The oxygenation of the atmosphere and oceans. *Phil. Trans. R. Soc. B Biol. Sci.* 361, 903–915. <https://doi.org/10.1098/rstb.2006.1838>.
- Holland, H.D., 1984. *The chemical evolution of the atmosphere and oceans*. Princeton University Press.
- Imachi, H., Nobu, M.K., Nakahara, N., Morono, Y., Ogawara, M., Takaki, Y., Takano, Y., Uematsu, K., Ikuta, T., Ito, M., Matsui, Y., Miyazaki, M., Murata, K., Saito, Y., Sakai, S., Song, C., Tasumi, E., Yamanaka, Y., Yamaguchi, T., Kamagata, Y., Tamaki, H., Takai, K., 2019. Isolation of an archaeon at the prokaryote-eukaryote interface. *bioRxiv* 726976. <https://doi.org/10.1101/726976>.
- Isson, T.T., Love, G.D., Dupont, C.L., Reinhard, C.T., Zumberge, A.J., Asael, D., Gueguen, B., McCrow, J., Gill, B.C., Owens, J., Rainbird, R.H., Rooney, A.D., Zhao, M.Y., Stueeken, E.E., Konhauser, K.O., John, S.G., Lyons, T.W., Planavsky, N.J., 2018. Tracking the rise of eukaryotes to ecological dominance with zinc isotopes. *Geobiology* 16, 341–352. <https://doi.org/10.1111/gbi.12289>.
- Izon, G., Luo, G., Uveges, B.T., Beukes, N., Kitajima, K., Ono, S., Valley, J.W., Ma, X., Summons, R.E., 2022. Bulk and grain-scale minor sulfur isotope data reveal complexities in the dynamics of Earth's oxygenation. *Proc. Natl. Acad. Sci. U. S. A.* 119, e2025606119 https://doi.org/10.1073/PNAS.2025606119/SUPPL_FILE/PNAS.2025606119.S004.XLSX.
- Jabłońska, J., Tawfik, D.S., 2021. The evolution of oxygen-utilizing enzymes suggests early biosphere oxygenation. *Nat. Ecol. Evol.* 5 (4), 442–448. <https://doi.org/10.1038/s41559-020-01386-9>.
- Javaux, E.J., Knoll, A.H., Walter, M.R., 2004. TEM evidence for eukaryotic diversity in mid-Proterozoic oceans. *Geobiology* 2, 121–132. <https://doi.org/10.1111/J.1472-4677.2004.00027.X>.
- Javaux, E.J., Lepot, K., 2018. The Paleoproterozoic fossil record: Implications for the evolution of the biosphere during Earth's middle-age. *Earth Sci. Rev.* 176, 68–86. <https://doi.org/10.1016/j.earscirev.2017.10.001>.
- Johnson, C.M., Zheng, X.Y., Djokic, T., van Kranendonk, M.J., Czaja, A.D., Roden, E.E., Beard, B.L., 2022. Early Archean biogeochemical iron cycling and nutrient availability: New insights from a 3.5 Ga land-sea transition. *Earth Sci. Rev.* 228, 103992 <https://doi.org/10.1016/j.earscirev.2022.103992>.
- Jones, C., Nomosatryo, S., Crowe, S.A., Bjerrum, C.J., Canfield, D.E., 2015. Iron oxides, divalent cations, silica, and the early earth phosphorus crisis. *Geology* 43, 135–138. <https://doi.org/10.1130/G36044.1>.
- Karhu, J.A., Holland, H.D., 1996. Carbon isotopes and the rise of atmospheric oxygen. *Geology* 24, 867–870. [https://doi.org/10.1130/0091-7613\(1996\)024<0867:CIATRO>2.3.CO;2](https://doi.org/10.1130/0091-7613(1996)024<0867:CIATRO>2.3.CO;2).
- Kasten, S., Jørgensen, B.B., 2000. Sulfate reduction in marine sediments. In: *Marine Geochemistry*. Springer, Berlin Heidelberg, pp. 263–281. https://doi.org/10.1007/978-3-662-04242-7_8.
- Kendall, B., Reinhard, C.T., Lyons, T.W., Kaufman, A.J., Poulton, S.W., Anbar, A.D., 2010. Pervasive oxygenation along late Archean Ocean margins. *Nat. Geosci.* 3, 647–652. <https://doi.org/10.1038/ngeo942>.
- Killingsworth, B.A., Sansjofre, P., Philippot, P., Cartigny, P., Thomazo, C., Lalonde, S.V., 2019. Constraining the rise of oxygen with oxygen isotopes. *Nat. Commun.* 10, 1–10. <https://doi.org/10.1038/s41467-019-12883-2>.
- Kimura, H., Watanabe, Y., 2001. Oceanic anoxia at the Precambrian-Cambrian boundary. *Geology* 29, 995–998.
- Kipp, M.A., Stüeken, E.E., 2017. Biomass recycling and Earth's early phosphorus cycle. *Sci. Adv.* 3, 1–7. <https://doi.org/10.1126/sciadv.aao4795>.
- Kipp, M.A., Stüeken, E.E., Bekker, A., Buick, R., 2017. Selenium isotopes record extensive marine suboxia during the Great Oxidation Event. *Proc. Natl. Acad. Sci. U. S. A.* 114, 875–880. https://doi.org/10.1073/PNAS.1615867114/SUPPL_FILE/PNAS.1615867114.SD01.XLSX.
- Kipp, M.A., Stüeken, E.E., Yun, M., Bekker, A., Buick, R., 2018. Pervasive aerobic nitrogen cycling in the surface ocean across the Paleoproterozoic Era. *Earth Planet. Sci. Lett.* 500, 117–126. <https://doi.org/10.1016/j.epsl.2018.08.007>.
- Knoll, A.H., 2011. The multiple origins of complex multicellularity. *Annu. Rev. Earth Planet. Sci.* 39, 217–239. <https://doi.org/10.1146/annurev.earth.031208.100209>.
- Knoll, A.H., Canfield, D.E., Konhauser, K.O., 2012. *Fundamentals of Geobiology*. John Wiley & Sons, Ltd, Chichester, UK. <https://doi.org/10.1002/9781118280874>.
- Knoll, A.H., Javaux, E.J., Hewitt, D., Cohen, P., 2006. Eukaryotic organisms in Proterozoic oceans. *Phil. Trans. R. Soc. B Biol. Sci.* 361, 1023–1038. <https://doi.org/10.1098/RSTB.2006.1843>.
- Knoll, A.H., Nowak, M.A., 2017. The timetable of evolution. *Sci. Adv.* <https://doi.org/10.1126/sciadv.1603076>.
- Knoll, A.H., Sperling, E.A., 2014. Oxygen and animals in Earth history. *Proc. Natl. Acad. Sci. U. S. A.* 111, 3907–3908. <https://doi.org/10.1073/PNAS.1401745111/ASSET/612DDC0B-BDD6-4951-8A4A-D112B062A4BC/ASSETS/PNAS.1401745111.FP.PNG>.
- Konhauser, K.O., Lalonde, S.V., Planavsky, N.J., Pecoits, E., Lyons, T.W., Mojzsis, S.J., Rouxel, O.J., Barley, M.E., Rosiere, C., Fralick, P.W., Kump, L.R., Bekker, A., 2011. Aerobic bacterial pyrite oxidation and acid rock drainage during the Great Oxidation Event. *Nature* 478, 369–373. <https://doi.org/10.1038/nature10511>.
- Ku, C., Martin, W.F., 2016. A natural barrier to lateral gene transfer from prokaryotes to eukaryotes revealed from genomes: the 70 % rule. *BMC Biol.* 14, 89. <https://doi.org/10.1186/s12915-016-0315-9>.
- Ku, C., Nelson-Sathi, S., Roettger, M., Sousa, F.L., Lockhart, P.J., Bryant, D., Hazkani-Covo, E., McInerney, J.O., Landan, G., Martin, W.F., 2015. Endosymbiotic origin and differential loss of eukaryotic genes. *Nature* 524, 427–432. <https://doi.org/10.1038/nature14963>.
- Kuang, H., Bai, H., Peng, N., Qi, K., Wang, Y., Chen, X., Liu, Y., 2022. Temporal and spatial distribution of Precambrian red beds and their formation mechanisms. *Geosyst. Geoenviron.* 1, 100098 <https://doi.org/10.1016/j.GEOGEO.2022.100098>.
- Kump, L.R., Arthur, M.A., 1999. Interpreting carbon-isotope excursions: Carbonates and organic matter. *Chem. Geol.* 161, 181–198. [https://doi.org/10.1016/S0009-2541\(99\)00086-8](https://doi.org/10.1016/S0009-2541(99)00086-8).
- Kump, L.R., Seyfried, W.E., 2005. Hydrothermal Fe fluxes during the Precambrian: effect of low oceanic sulfate concentrations and low hydrostatic pressure on the composition of black smokers. *Earth Planet. Sci. Lett.* 235, 654–662. <https://doi.org/10.1016/j.epsl.2005.04.040>.
- Laakso, T.A., Schrag, D.P., 2019. A small marine biosphere in the Proterozoic. *Geobiology* 17, 161–171. <https://doi.org/10.1111/gbi.12323>.
- Laakso, T.A., Schrag, D.P., 2017. A theory of atmospheric oxygen. *Geobiology* 15, 366–384. <https://doi.org/10.1111/gbi.12230>.
- Lamb, D.M., Awramik, S.M., Chapman, D.J., Zhu, S., 2009. Evidence for eukaryotic diversification in the ~1800 million-year-old Changzhougou Formation, North China. *Precambrian Res.* 173, 93–104. <https://doi.org/10.1016/j.precamres.2009.05.005>.
- Lenton, T.M., Boyle, R.A., Poulton, S.W., Shields-Zhou, G.A., Butterfield, N.J., 2014. Co-evolution of eukaryotes and ocean oxygenation in the Neoproterozoic era. *Nat. Geosci.* 7, 257–265. <https://doi.org/10.1038/ngeo2108>.
- Lenton, T.M., Daines, S.J., 2018. The effects of marine eukaryote evolution on phosphorus, carbon and oxygen cycling across the Proterozoic-Phanerozoic transition. *Emerg. Top Life Sci.* 2, 267–278. <https://doi.org/10.1042/etls20170156>.
- Lindwiark, G., Muller, M., 1973. A Cytoplasmic Organelle Flagellate Trichomonas foetus, and its Role in Puvrate Metabolism *. *Biol. Chem.* 248, 7724–7728.

- Liu, H., Zartman, R.E., Ireland, T.R., Sun, W., dong, 2019. Global atmospheric oxygen variations recorded by Th/U systematics of igneous rocks. *Proc. Natl. Acad. Sci. USA* 116, 18854–18859. https://doi.org/10.1073/PNAS.1902833116/SUPPL_FILE/PNAS.1902833116.SD02.TXT.
- Liu, P., Liu, J., Ji, A., Reinhard, C.T., Planavsky, N.J., Babikov, D., Najjar, R.G., Kasting, J.F., 2021. Triple oxygen isotope constraints on atmospheric O₂ and biological productivity during the mid-Proterozoic. *Proc. Natl. Acad. Sci. U. S. A.* 118, e2105074118 https://doi.org/10.1073/PNAS.2105074118/SUPPL_FILE/PNAS.2105074118.SAPP.PDF.
- Logan, G.A., Hayes, J.M., Hieshima, G.B., Summons, R.E., 1995. Terminal Proterozoic reorganization of biogeochemical cycles. *Nature* 376, 53–56. <https://doi.org/10.1038/376053a0>.
- Loron, C., Moczyłowska, M., 2017. Tonian (Neoproterozoic) eukaryotic and prokaryotic organic-walled microfossils from the upper Visingsö Group, Sweden, 42, 220–254. <https://doi.org/10.1080/01916122.2017.1335656>.
- Loron, C.C., François, C., Rainbird, R.H., Turner, E.C., Borszajn, S., Javaux, E.J., 2019. Early fungi from the Proterozoic era in Arctic Canada. *Nature* 570 (7760), 232–235. <https://doi.org/10.1038/s41586-019-1217-0>.
- Lu, Z., Jenkyns, H.C., Rickaby, R.E.M., 2010. Iodine to calcium ratios in marine carbonate as a paleo-redox proxy during oceanic anoxic events. *Geology* 38, 1107–1110. <https://doi.org/10.1130/G31145.1>.
- Luther, G.W., Campbell, T., 1991. Iodine speciation in the water column of the Black Sea. *Deep Sea Research Part A: Oceanogr. Res. Papers* 38, S875–S882. [https://doi.org/10.1016/S0198-0149\(10\)80014-7](https://doi.org/10.1016/S0198-0149(10)80014-7).
- Luz, B., Barkan, E., Bender, M.L., Thieme, M.H., Boering, K.A., 1999. Triple-isotope composition of atmospheric oxygen as a tracer of biosphere productivity. *Nature* 400, 547–550. <https://doi.org/10.1038/22987>.
- Lyons, T.W., Diamond, C.W., Planavsky, N.J., Reinhard, C.T., Li, C., 2021. Oxygenation, Life, and the Planetary System during Earth's Middle history: an Overview. *Astrobiology* 21, 906–923. <https://doi.org/10.1089/AST.2020.2418/ASSET/IMAGES/LARGE/AST.2020.2418.FIGURE3.JPEG>.
- Lyons, T.W., Reinhard, C.T., Planavsky, N.J., 2014. The rise of oxygen in Earth's early ocean and atmosphere. *Nature* 506, 307–315. <https://doi.org/10.1038/nature13068>.
- Magnabosco, C., Moore, K.R., Wolfe, J.M., Fournier, G.P., 2018. Dating phototrophic microbial lineages with reticulate gene histories. *Geobiology* 16, 179–189. <https://doi.org/10.1111/gbi.12273>.
- Mänd, K., Planavsky, N.J., Porter, S.M., Robbins, L.J., Wang, C., Kreitsmann, T., Paiste, K., Paiste, P., Romashkin, A.E., Deines, Y.E., Kirsimäe, K., Lepland, A., Konhauser, K.O., 2022. Chromium evidence for protracted oxygenation during the Paleoproterozoic. *Earth Planet. Sci. Lett.* 584, 117501 <https://doi.org/10.1016/J.EPSL.2022.117501>.
- Martin, A.P., Condon, D.J., Prave, A.R., Lepland, A., 2013. A review of temporal constraints for the Palaeoproterozoic large, positive carbonate carbon isotope excursion (the Lomagundi-Jatuli Event). *Earth Sci. Rev.* <https://doi.org/10.1016/j.earscirev.2013.10.006>.
- Martin, W., Müller, M., 1998. The hydrogen hypothesis for the first eukaryote. *Nature*. <https://doi.org/10.1038/32096>.
- Martin, W.F., 2017. Physiology, anaerobes, and the origin of mitosing cells 50 years on. *J. Theor. Biol.* 434, 2–10. <https://doi.org/10.1016/j.jtbi.2017.01.004>.
- Mayika, K.B., Moussavou, M., Prave, A.R., Lepland, A., Mbina, M., Kirsimäe, K., 2020. The Paleoproterozoic Franciscan succession of Gabon and the Lomagundi-Jatuli event. *Geology* 48, 1099–1104. <https://doi.org/10.1130/G47651.1>.
- McDonnell, A.M.P., Buesseler, K.O., 2010. Variability in the average sinking velocity of marine particles. *Limnol. Oceanogr.* 55, 2085–2096. <https://doi.org/10.4319/L.2010.55.5.2085>.
- McKenzie, N.R., Horton, B.K., Loomis, S.E., Stockli, D.F., Planavsky, N.J., Lee, C.T.A., 2016. Continental arc volcanism as the principal driver of icehouse-greenhouse variability. *Science* 352, 444–447. <https://doi.org/10.1126/science.1257877>.
- McMahon, S., van Smeerdijk Hood, A., McIlroy, D., 2017. The origin and occurrence of subaqueous sedimentary cracks. In: Geological Society Special Publication. Geological Society of London, pp. 285–309. <https://doi.org/10.1144/SP448.15>.
- Melezhik, V.A., Huhma, H., Condon, D.J., Fallick, A.E., Whitehouse, M.J., 2007. Temporal constraints on the Paleoproterozoic Lomagundi-Jatuli carbon isotopic event. *Geology* 35, 655–658. <https://doi.org/10.1130/G23764A.1>.
- Miao, L., Moczyłowska, M., Zhu, S., Zhu, M., 2019. New record of organic-walled, morphologically distinct microfossils from the late Paleoproterozoic Changcheng Group in the Yanshan Range, North China. *Precambrian Res.* 321, 172–198. <https://doi.org/10.1016/J.PRECAMRES.2018.11.019>.
- Mills, D.B., Boyle, R.A., Daines, S.J., Sperling, E.A., Pisani, D., Donoghue, P.C.J., Lenton, T.M., 2022. Eukaryogenesis and oxygen in Earth history. *Nat. Ecol. Evol.* 6 (5), 520–532. <https://doi.org/10.1038/s41559-022-01733-y>.
- Mitchell, R.L., Sheldon, N.D., 2010. The ~1100Ma Sturgeon Falls paleosol revisited: Implications for Mesoproterozoic weathering environments and atmospheric CO₂ levels. *Precambrian Res.* 183, 738–748. <https://doi.org/10.1016/j.precamres.2010.09.003>.
- Mitchell, R.L., Sheldon, N.D., 2009. Weathering and paleosol formation in the 1.1 Ga Keweenaw Rift. *Precambrian Res.* 168, 271–283. <https://doi.org/10.1016/j.precamres.2008.09.013>.
- Miyazaki, Y., Planavsky, N.J., Bolton, E.W., Reinhard, C.T., 2018. Making sense of massive Carbon Isotope Excursions with an Inverse Carbon Cycle Model. *J. Geophys. Res. Biogeosci.* 123, 2485–2496. <https://doi.org/10.1029/2018JG004416>.
- Moreira, D., López-García, P., 1998. Symbiosis between methanogenic archaea and δ -proteobacteria as the origin of eukaryotes: the syntrophic hypothesis. *J. Mol. Evol.* 47, 517–530. <https://doi.org/10.1007/PL00006408>.
- Morris, S.C., 2002. Ancient animals or something else entirely? *Science* 298. <https://doi.org/10.1126/science.298.5591.57c>, 57.3–58.
- Müller, M., Mentel, M., van Hellemond, J.J., Henze, K., Woehle, C., Gould, S.B., Yu, R.-Y., van der Giezen, M., Tielens, A.G.M., Martin, W.F., 2012. Biochemistry and Evolution of Anaerobic Energy Metabolism in Eukaryotes. *Microbiol. Mol. Biol. Rev.* 76, 444–495. <https://doi.org/10.1128/mmb.05024-11>.
- Och, L.M., Shields-Zhou, G.A., 2012. The Neoproterozoic oxygenation event: Environmental perturbations and biogeochemical cycling. *Earth Sci. Rev.* <https://doi.org/10.1016/j.earscirev.2011.09.004>.
- Ohmoto, H., Watanabe, Y., Ikemi, H., Poulson, S.R., Taylor, B.E., 2006. Sulphur isotope evidence for anoxic Archean atmosphere. *Nature* 442, 908–911. <https://doi.org/10.1038/nature05044>.
- Olson, S.L., Kump, L.R., Kasting, J.F., 2013. Quantifying the areal extent and dissolved oxygen concentrations of Archean oxygen oases. *Chem. Geol.* 362, 35–43. <https://doi.org/10.1016/j.chemgeo.2013.08.012>.
- Olson, S.L., Ostrander, C.M., Gregory, D.D., Roy, M., Anbar, A.D., Lyons, T.W., 2019. Volcanically modulated pyrite burial and ocean-atmosphere oxidation. *Earth Planet. Sci. Lett.* 506, 417–427. <https://doi.org/10.1016/J.EPSL.2018.11.015>.
- Ossa Ossa, F., Hofmann, A., Vidal, O., Kramers, J.D., Belyanin, G., Cavalazzi, B., 2016. Unusual manganese enrichment in the Mesoarchean Mozaan Group, Pongola Supergroup, South Africa. *Precambrian Res.* 281, 414–433. <https://doi.org/10.1016/J.PRECAMRES.2016.06.009>.
- Ossa Ossa, F., Hofmann, A., Wille, M., Spangenberg, J.E., Bekker, A., Poulton, S.W., Eickmann, B., Schoenberg, R., 2018. Aerobic iron and manganese cycling in a redox-stratified Mesoarchean epicontinental sea. *Earth Planet. Sci. Lett.* 500, 28–40. <https://doi.org/10.1016/j.epsl.2018.07.044>.
- Ossa Ossa, F., Spangenberg, J.E., Bekker, A., König, S., Stüeken, E.E., Hofmann, A., Poulton, S.W., Yierpan, A., Varas-Reus, M.I., Eickmann, B., Andersen, M.B., Schoenberg, R., 2022. Moderate levels of oxygenation during the late stage of Earth's Great Oxidation Event. *Earth Planet. Sci. Lett.* 594, 117716 <https://doi.org/10.1016/J.EPSL.2022.117716>.
- Ostrander, C.M., Johnson, A.C., Anbar, A.D., 2021. Earth's First Redox Revolution. *Ann. Rev. Earth Planet. Sci.* 49, 337–366. <https://doi.org/10.1146/ANNUREV-EARTH-072020-055249>.
- Ostrander, C.M., Nielsen, S.G., Owens, J.D., Kendall, B., Gordon, G.W., Romaniello, S.J., Anbar, A.D., 2019. Fully oxygenated water columns over continental shelves before the Great Oxidation Event. *Nat. Geosci.* 12, 186–192. <https://doi.org/10.1038/s41561-019-0309-7>.
- Ozaki, K., Reinhard, C.T., Tajika, E., 2019. A sluggish mid-Proterozoic biosphere and its effect on Earth's redox balance. *Geobiology* 17, 3–11. <https://doi.org/10.1111/gbi.12317>.
- Pack, A., Höweling, A., Hezel, D.C., Stefanak, M.T., Beck, A.K., Peters, S.T.M., Sengupta, S., Herwartz, D., Folco, L., 2017. Tracing the oxygen isotope composition of the upper Earth's atmosphere using cosmic spherules. *Nat. Commun.* 8 (1), 1–7. <https://doi.org/10.1038/ncomms15702>.
- Pang, K., Tang, Q., Yuan, X.L., Wan, B., Xiao, S., 2015. A biomechanical analysis of the early eukaryotic fossil Valeria and new occurrence of organic-walled microfossils from the Paleo-Mesoproterozoic Ruyang Group. *Palaeoworld* 24, 251–262. <https://doi.org/10.1016/j.palwor.2015.04.002>.
- Parfrey, L.W., Lahr, D.J.G., Knoll, A.H., Katz, L.A., 2011. Estimating the timing of early eukaryotic diversification with multigene molecular clocks. *Proc. Natl. Acad. Sci. U. S. A.* 108, 13624–13629. <https://doi.org/10.1073/pnas.1110633108>.
- Partin, C.A., Bekker, A., Planavsky, N.J., Scott, C.T., Gill, B.C., Li, C., Podkovyrov, V., Maslov, A., Konhauser, K.O., Lalonde, S.V., Love, G.D., Poulton, S.W., Lyons, T.W., 2013. Large-scale fluctuations in Precambrian atmospheric and oceanic oxygen levels from the record of U in shales. *Earth Planet. Sci. Lett.* 369–370, 284–293. <https://doi.org/10.1016/J.EPSL.2013.03.031>.
- Pavlov, A.A., Kasting, J.F., 2002. Mass-independent fractionation of sulfur isotopes in Archean sediments: strong evidence for an anoxic Archean atmosphere. *Astrobiology* 2, 27–41. <https://doi.org/10.1089/153110702753621321>.
- Peng, Y., Bao, H., Yuan, X., 2009. New morphological observations for Paleoproterozoic acritarchs from the Chuanlinggou Formation, North China. *Precambrian Res.* 168, 223–232. <https://doi.org/10.1016/j.precamres.2008.10.005>.
- Pertunnen, V., Vaasjoki, M., 2001. U-Pb geochronology of the Peräpohja Schist Belt, northwestern Finland. *Spec. Pap. Geol. Surv. Finland* 45–84.
- Philippot, P., Ávila, J.N., Killingsworth, B.A., Tessalina, S., Baton, F., Caquineau, T., Muller, E., Pecoits, E., Cartigny, P., Lalonde, S.V., Ireland, T.R., Thomazo, C., Van Kranendonk, M.J., Busigny, V., 2018. Globally asynchronous Sulphur isotope signals require re-definition of the Great Oxidation Event. *Nat. Commun.* 9 <https://doi.org/10.1038/s41467-018-04621-x>.
- Planavsky, N.J., Asael, D., Hofmann, A., Reinhard, C.T., Lalonde, S.V., Knudsen, A., Wang, X., Ossa Ossa, F., Pecoits, E., Smith, A.J.B., Beukes, N.J., Bekker, A., Johnson, T.M., Konhauser, K.O., Lyons, T.W., Rouxel, O.J., 2014. Evidence for oxygenic photosynthesis half a billion years before the Great Oxidation Event. *Nat. Geosci.* 7, 283–286. <https://doi.org/10.1038/ng eo2122>.
- Planavsky, N.J., Asael, D., Rooney, A.D., Robbins, L.J., Gill, B.C., Dehler, C.M., Cole, D. B., Porter, S.M., Love, G.D., Konhauser, K.O., Reinhard, C.T., 2022a. A sedimentary record of the evolution of the global marine phosphorus cycle. *Geobiology*. <https://doi.org/10.1111/GBI.12536>.
- Planavsky, N.J., Bekker, A., Hofmann, A., Owens, J.D., Lyons, T.W., 2012. Sulfur record of rising and falling marine oxygen and sulfate levels during the Lomagundi event. *Proc. Natl. Acad. Sci. U. S. A.* 109, 18300–18305. <https://doi.org/10.1073/pnas.1120387109/-/DCSupplemental>.
- Planavsky, N.J., Cole, D.B., Isson, T.T., Reinhard, C.T., Crockford, P.W., Sheldon, N.D., Lyons, T.W., 2018. A case for low atmospheric oxygen levels during Earth's middle history. *Emerg. Top Life Sci.* 2, 149–159. <https://doi.org/10.1042/etls20170161>.

- Planavsky, N.J., Fakhraee, M., Bolton, E.W., Reinhard, C.T., Isson, T.T., Zhang, S., Mills, B.J.W., 2022b. On carbon burial and net primary production through Earth's history. *Am. J. Sci.* 322, 413–460. <https://doi.org/10.2475/03.2022.01>.
- Planavsky, N.J., McGoldrick, P., Scott, C.T., Li, C., Reinhard, C.T., Kelly, A.E., Chu, X., Bekker, A., Love, G.D., Lyons, T.W., 2011. Widespread iron-rich conditions in the mid-Proterozoic Ocean. *Nature* 477, 448–451. <https://doi.org/10.1038/nature10327>.
- Planavsky, N.J., Reinhard, C.T., Wang, X., Thomson, D., McGoldrick, P., Rainbird, R.H., Johnson, T., Fischer, W.W., Lyons, T.W., 2014b. Low mid-proterozoic atmospheric oxygen levels and the delayed rise of animals. *Science* 346, 635–638. <https://doi.org/10.1126/science.1258410>.
- Pogge Von Strandmann, P.A.E., Stüeken, E.E., Elliott, T., Poulton, S.W., Dehler, C.M., Canfield, D.E., Catling, D.C., 2015. Selenium isotope evidence for progressive oxidation of the Neoproterozoic biosphere. *Nat. Commun.* 6 (1), 1–10. <https://doi.org/10.1038/ncomms10157>.
- Porter, S., 2011. The rise of predators. *Geology*. <https://doi.org/10.1130/focus062011.1>.
- Porter, S.M., 2020. Insights into eukaryogenesis from the fossil record. *Interf. Focus* 10. <https://doi.org/10.1098/RSFS.2019.0105>.
- Porter, S.M., Agić, H., Riedman, L.A., 2018. Anoxic ecosystems and early eukaryotes. *Emerg. Top. Life Sci.* 2, 299–309. <https://doi.org/10.1042/etls20170162>.
- Poulton, S.W., Bekker, A., Cumming, V.M., Zerkle, A.L., Canfield, D.E., Johnston, D.T., 2021. A 200-million-year delay in permanent atmospheric oxygenation. *Nature* 592 (7853), 232–236. <https://doi.org/10.1038/s41586-021-03393-7>.
- Prave, A.R., Kirsinmäe, K., Leland, A., Fallick, A.E., Kreitsmann, T., Deines, Y.E., Romashkin, A.E., Rychanchik, D.V., Medvedev, P.V., Moussavou, M., Bakakas, K., Hodgskiss, M.S.W., 2022. The grandest of them all: the Lomagundi-Jatuli Event and Earth's oxygenation. *J. Geol. Soc. Lond.* 179. <https://doi.org/10.1144/JGS2021-036>.
- Rasmussen, B., Bengtson, S., Fletcher, I.R., McNaughton, N.J., 2002. Discoidal impressions and trace-like fossils more than 1200 million years old. *Science* 296 (5926), 1112–1115. <https://doi.org/10.1126/science.1070166>.
- Rasmussen, B., Fletcher, I.R., Brooks, J.J., Kilburn, M.R., 2008. Reassessing the first appearance of eukaryotes and cyanobacteria. *Nature* 455, 1101–1104. <https://doi.org/10.1038/nature07381>.
- Rasmussen, B., Muhling, J.R., 2019. Syn-tectonic hematite growth in Paleoproterozoic Stirling Range “red beds”, Albany-Fraser Orogen, Australia: evidence for oxidation during late-stage orogenic uplift. *Precambrian Res.* 321, 54–63. <https://doi.org/10.1016/j.precamres.2018.12.002>.
- Reinhard, C.T., Planavsky, N.J., Gill, B.C., Ozaki, K., Robbins, L.J., Lyons, T.W., Fischer, W.W., Wang, C., Cole, D.B., Konhauser, K.O., 2017. Evolution of the global phosphorus cycle, 541, 386–389. <https://doi.org/10.1038/nature20772>.
- Reinhard, C.T., Planavsky, N.J., Lyons, T.W., 2013. Long-term sedimentary recycling of rare Sulphur isotope anomalies. *Nature* 497, 100–103. <https://doi.org/10.1038/nature12021>.
- Roscoe, S.M., 1969. Huronian rocks and uraniferous conglomerates in the Canadian Shield. *Can. Geol. Surv. Paper* 68, 205.
- Sagan, L., 1967. On the origin of mitosing cells. *J. Theor. Biol.* 14. [https://doi.org/10.1016/0022-5193\(67\)90079-3](https://doi.org/10.1016/0022-5193(67)90079-3).
- Schidlowski, M., Eichmann, R., Junge, C.E., 1976. Carbon isotope geochemistry of the Precambrian Lomagundi carbonate province, Rhodesia. *Geochim. Cosmochim. Acta* 40, 449–455. [https://doi.org/10.1016/0016-7037\(76\)90010-7](https://doi.org/10.1016/0016-7037(76)90010-7).
- Schwieterman, E.W., Kiang, N.Y., Parenteau, M.N., Harman, C.E., Dassarma, S., Fisher, T.M., Arney, G.N., Hartnett, H.E., Reinhard, C.T., Olson, S.L., Meadows, V.S., Cockell, C.S., Walker, S.L., Grenfell, J.L., Hegde, S., Rugheimer, S., Hu, R., Lyons, T.W., 2018. Exoplanet Biosignatures: a Review of Remotely Detectable signs of Life. *Astrobiology*. <https://doi.org/10.1089/ast.2017.1729>.
- Scott, C., Wing, B.A., Bekker, A., Planavsky, N.J., Medvedev, P., Bates, S.M., Yun, M., Lyons, T.W., 2014. Pyrite multiple-sulfur isotope evidence for rapid expansion and contraction of the early Paleoproterozoic seawater sulfate reservoir. *Earth Planet. Sci. Lett.* 389, 95–104. <https://doi.org/10.1016/j.epsl.2013.12.010>.
- Seilacher, A., 2007. *Trace fossil analysis*. Springer.
- Shen, Y., Knoll, A.H., Walter, M.R., 2003. Evidence for low sulphate and anoxia in a mid-Proterozoic marine basin. *Nature* 423, 632–635. <https://doi.org/10.1038/nature01651>.
- Shields-Zhou, G., Och, L., 2011. The case for a neoproterozoic oxygenation event: Geochemical evidence and biological consequences. *GSA Today* 21, 4–11. <https://doi.org/10.1130/GSATG102A.1>.
- Shih, P.M., Matzke, N.J., 2013. Primary endosymbiosis events date to the later Proterozoic with cross-calibrated phylogenetic dating of duplicated ATPase proteins. *Proc. Natl. Acad. Sci. U. S. A.* 110, 12355–12360. <https://doi.org/10.1073/PNAS.1305813110/-DCSUPPLEMENTAL/SAPP.PDF>.
- Slotnick, S.P., Johnson, J.E., Rasmussen, B., Raub, T.D., Webb, S.M., Zi, J.W., Kirschvink, J.L., Fischer, W.W., 2022. Reexamination of 2.5-Ga “whiff” of oxygen interval points to anoxic ocean before GOE. *Sci. Adv.* 8, 7190. https://doi.org/10.1126/SCIADV.ABJ7190/SUPPL_FILE/SCIADV.ABJ7190.DATASET.S1.ZIP.
- Soo, R.M., Hemp, J., Parks, D.H., Fischer, W.W., Hugenholtz, P., 2017. On the origins of oxygenic photosynthesis and aerobic respiration in Cyanobacteria. *Science* 355 (6400), 1436–1440. <https://doi.org/10.1126/science.1258410>.
- Spang, A., Stairs, C.W., Dombrowski, N., Eme, L., Lombard, J., Caceres, E.F., Greening, C., Baker, B.J., Ettema, T.J.G., 2019. Proposal of the reverse flow model for the origin of the eukaryotic cell based on comparative analyses of Asgard archaeal metabolism. *Nat. Microbiol.* 4, 1138–1148. <https://doi.org/10.1038/s41564-019-0406-9>.
- Sperling, E.A., Wolock, C.J., Morgan, A.S., Gill, B.C., Kunzmann, M., Halverson, G.P., Macdonald, F.A., Knoll, A.H., Johnston, D.T., 2015. Statistical analysis of iron geochemical data suggests limited late Proterozoic oxygenation. *Nature* 523 (7561), 451–454. <https://doi.org/10.1038/nature14589>.
- Stairs, C.W., Leger, M.M., Roger, A.J., 2015. Diversity and origins of anaerobic metabolism in mitochondria and related organelles. *Phil. Trans. R. Soc. B Biol. Sci.* <https://doi.org/10.1098/rstb.2014.0326>.
- Stamati, K., Mudera, V., Cheema, U., 2011. Discovery of oxygen Evolution of oxygen utilization in multicellular organisms and implications for cell signalling in tissue engineering Article. *J. Tissue Eng.* 2. <https://doi.org/10.1177/2041731411432365>.
- Stüeken, E.E., Buick, R., Guy, B.M., Koehler, M.C., 2015. Isotopic evidence for biological nitrogen fixation by molybdenum-nitrogenase from 3.2 Gyr. *Nature* 520 (7549), 666–669. <https://doi.org/10.1038/nature14180>.
- Stüeken, E.E., Kipp, M.A., Koehler, M.C., Buick, R., 2016. The evolution of Earth's biogeochemical nitrogen cycle. *Earth Sci. Rev.* 160, 220–239. <https://doi.org/10.1016/J.EARSCIREV.2016.07.007>.
- Swart, P.K., 2015. The geochemistry of carbonate diagenesis: the past, present and future. *Sedimentology* 62, 1233–1304. <https://doi.org/10.1111/SED.12205>.
- Swart, P.K., Eberli, G., 2005. The nature of the $\delta^{13}\text{C}$ of periplatform sediments: Implications for stratigraphy and the global carbon cycle. *Sediment. Geol.* 175, 115–129. <https://doi.org/10.1016/J.SEDGEO.2004.12.029>.
- Tang, D., Shi, X., Wang, X., Jiang, G., 2016. Extremely low oxygen concentration in mid-Proterozoic shallow seawaters. *Precambrian Res.* 276, 145–157. <https://doi.org/10.1016/j.precamres.2016.02.005>.
- Tang, Q., Pang, K., Yuan, X., Xiao, S., 2020. A one-billion-year-old multicellular chlorophyte. *Nat. Ecol. Evol.* 4 (4), 543–549. <https://doi.org/10.1038/s41559-020-1122-9>.
- Tarhan, L.G., Droser, M.L., Planavsky, N.J., Johnston, D.T., 2015. Protracted development of bioturbation through the early Palaeozoic Era. *Nat. Geosci.* 8 (11), 865–869. <https://doi.org/10.1038/ngeo2537>.
- Thiemens, M.H., 2006. History and applications of mass-independent isotope effects. *Annu. Rev. Earth Planet. Sci.* 34, 217–262. <https://doi.org/10.1146/annurev.earth.34.031405.125026>.
- Thiemens, M.H., Heidenreich, J.E., 1983. The mass-independent fractionation of oxygen: a novel isotope effect and its possible cosmochemical implications. *Science* 219 (5219), 1073–1075. <https://doi.org/10.1126/science.219.4588.1073>.
- Tice, M.M., Lowe, D.R., 2004. Photosynthetic microbial mats in the 3,416-Myr-old Ocean. *Nature* 431, 549–552. <https://doi.org/10.1038/nature02888>.
- Tria, F.D.K., Brueckner, J., Skejo, J., Xavier, J.C., Kapust, N., Knopp, M., Wimmer, J.L.E., Nagies, F.S.P., Zimorski, V., Gould, S.B., Garg, S.G., Martin, W.F., 2021. Gene Duplications Trace Mitochondria to the Onset of Eukaryote Complexity. *Genome Biol. Evol.* 13. <https://doi.org/10.1093/GBE/EBAB055>.
- Tyrrell, T., 1999. The relative influences of nitrogen and phosphorus on oceanic primary production. *Nature* 400 (6744), 525–531. <https://doi.org/10.1038/22941>.
- Tziperman, E., Halevy, I., Johnston, D.T., Knoll, A.H., Schrag, D.P., 2011. Biologically induced initiation of neoproterozoic snowball-earth events. *Proc. Natl. Acad. Sci. U. S. A.* 108, 15091–15096. <https://doi.org/10.1073/PNAS.1016361108>.
- Uveges, B.T., Izon, G., Ono, S., Beukes, N.J., Summons, R.E., 2023. Reconciling discrepant minor sulfur isotope records of the Great Oxidation Event. *Nat. Commun.* 14 (1), 1–12. <https://doi.org/10.1038/s41467-023-35820-w>. Royal Society.
- Wacey, D., Kilburn, M., Stoakes, C., Aggleton, H., Brasier, M., 2008. Ambient inclusion trails: their recognition, age range and applicability to early life on earth. *Mod. Approach. Solid Earth Sci.* 4, 113–134. https://doi.org/10.1007/978-1-4020-8306-8_3/COVER.
- Wallace, M.W., Hood, A., Shuster, A., Greig, A., Planavsky, N.J., Reed, C.P., 2017. Oxygenation history of the Neoproterozoic to early Phanerozoic and the rise of land plants. *Earth Planet. Sci. Lett.* 466, 12–19. <https://doi.org/10.1016/J.EPSL.2017.02.046>.
- Wang, C., Lechte, M.A., Reinhard, C.T., Asael, D., Cole, D.B., Halverson, G.P., Porter, S.M., Galili, N., Halevy, I., Rainbird, R.H., Lyons, T.W., Planavsky, N.J., 2022. Strong evidence for a weakly oxygenated ocean-atmosphere system during the Proterozoic. *Proc. Natl. Acad. Sci. U. S. A.* 119, e2116101119. https://doi.org/10.1073/PNAS.2116101119/SUPPL_FILE/PNAS.2116101119.SD04.XLSX.
- Ward, Bess B., Arp, Daniel J., Klotz, Martin G. (Eds.), 2011. *Nitrification*. American Society for Microbiology Press.
- Ward, L.M., Rasmussen, B., Fischer, W.W., 2019. Primary productivity was limited by electron donors prior to the advent of oxygenic photosynthesis. *J. Geophys. Res.* Biogeosci. 124, 211–226. <https://doi.org/10.1029/2018JG004679>.
- Wen, J., Thiemens, M.H., 1993. Multi-isotope study of the $\text{O}(1\text{D}) + \text{CO}_2$ exchange and stratospheric consequences. *J. Geophys. Res.* 98, 12801. <https://doi.org/10.1029/93JD00565>.
- Wilson, A.H., Zeh, A., 2018. U-Pb and Hf isotopes of detrital zircons from the Pongola Supergroup: Constraints on deposition ages, provenance and Archean evolution of the Kaapvaal craton. *Precambrian Res.* 305, 177–196. <https://doi.org/10.1016/J.PRECAMBRES.2017.12.020>.
- Wong, G.T.F., Brewer, P.G., 1977. The marine chemistry of iodine in anoxic basins. *Geochim. Cosmochim. Acta* 41, 151–159. [https://doi.org/10.1016/0016-7037\(77\)90195-8](https://doi.org/10.1016/0016-7037(77)90195-8).
- Zhao, A., 2009. Title Geochemistry of the Xiong'er volcanic rocks: implications for the Paleo-Mesoproterozoic accretion of the North China Craton. *Geochim. Cosmochim. Acta* 73, A1494–A1541. <https://doi.org/10.1016/j.gca.2009.05.019>.
- Zumberge, J.A., Love, G.D., Cárdenas, P., Sperling, E.A., Gunasekera, S., Rohrsen, M., Grosjean, E., Grotzinger, J.P., Summons, R.E., 2018. Demosponge steroid biomarker 26-methylstigmastane provides evidence for Neoproterozoic animals. *Nat. Ecol. Evol.* 2 (11), 1709–1714. <https://doi.org/10.1038/s41559-018-0676-2>.
- Zumberge, J.A., Rocher, D., Love, G.D., 2020. Free and kerogen-bound biomarkers from late Tonian sedimentary rocks record abundant eukaryotes in mid-Neoproterozoic marine communities. *Geobiology* 18, 326–347. <https://doi.org/10.1111/GBI.12378>.